# Wnt signaling regulates cytosolic translocation of Connexin 43

Xiaoming Hou[1,2¶], Mohammad R A Khan[3] , Mark Turmaine[4], Christopher Thrasivoulou[2] , David L Becker[2,5]and Aamir Ahmed[1,3]*

[1] Prostate Cancer Research Centre, 67 Riding House Street, Division of Surgery, University College London, London, W1W 7EJ, United Kingdom; [2]Research Department of Cell and Developmental Biology, The Centre for Cell and Molecular Dynamics, Rockefeller Building, University College London, London, WC1E 6JJ, United Kingdom; [3]Prostate Cancer Research Centre at the Centre for Stem Cells and Regenerative Medicine, King's College London, 28th Floor, Tower Wing, Guy's Hospital, Great Maze Pond, London SE1 9RT; [4]Division of Biosciences, University College London, Gower Street, London WC1E 6BT, United Kingdom; [5] Lee Kong Chian School of Medicine, Nanyang Technological University, 11, Mandalay Road, Singapore, 308232: Institute of Medical Biology, A*STAR, 8A- Biomedical Grove, Biopolis, Singapore 138648.

[¶]Current address: Department of Paediatrics, Provincial Hospital Affiliated to Shandong University, Jinan, PR China

*Corresponding author: Centre for Stem Cells and Regenerative Medicine, King's College London, 28th Floor, Tower Wing, Guy's Hospital, Great Maze Pond, London SE1 9RT
Telephone: +44 207188 7188 xtn 55708
Email: aamir.ahmed@kcl.ac.uk

**Abstract**

The availability of intracellular, stabilized ß-catenin, a transcription factor co-activator, is tightly regulated; ß-catenin is translocated into the nucleus in response to Wnt ligand binding to its cell membrane receptors. Here we show that Wnt signal activation in mammalian cells activates intracellular mobilization of Connexin 43 which belongs to a gap junction protein family, a new target protein in response to extracellular Wnt signal activation. Transmission electron microscopy (TEM) showed that the nuclear localization of Cx43 was increased by 8-10 fold in Wnt5A and 9B treated cells compared to controls; this Wnt induced increase was negated in the cells where Cx43 and ß-catenin were knocked down using shRNA. There was a significant ($p$<0.001) and concomitant depletion of the cell membrane and cytosolic signal of Cx43 in Wnt treated cells with an increase in the nuclear signal for Cx43; this was more obvious in cells where β-catenin was knocked down using shRNA. Conversely, Cx43 knockdown resulted in increased ß-catenin in the nucleus, in the absence of Wnt activation. Co-immunoprecipitation of Cx43 and ß-catenin proteins with a casein kinase (CKIδ) antibody showed that Cx43 interacts with ß-catenin and may form part of the so-called destruction complex. Functionally, Wnt activation increased the rate of wound re-epithelization in rat skin, *in vivo*.

## Introduction

The Wnt signaling pathway is known to play a key role in development (e.g. bone and limb morphogenesis) and disease (12), including cancer, osteoporosis and also in wound healing (54). There are two major intracellular transducers of Wnt signaling CTNNB1 (cadherin associated protein ß or ß-catenin, (34) and $Ca^{2+}$ (40); ß-catenin and CTNNB1 are used interchangeably in this manuscript). ß-catenin, was first discovered as a part of the adherent junction complex in the cell membranes of NIH 3T3 cell line (32). Wnt ligand binding to its plasma membrane receptor complex (5) activates intracellular calcium [Ca2+]i and desequesters and stabilizes ß-catenin from a multi-protein complex termed the ß-catenin destruction complex (44). Subsequent to its release from the destruction complex in the cytosol ß-catenin is translocated to the nucleus where it activates gene transcription in conjunction with LEF/TCF proteins (4). Recent studies have shown that, in mammalian cells, $Ca^{2+}$ and ß-catenin signaling act in a coordinated, interdependent manner (48). Whether Wnt signaling activation is involved in the translocation of a protein other than ß-catenin to the nucleus is not known. We demonstrate that Wnt signaling activation initiates translocation of at least one other protein, namely Connexin 43 (Cx43), a member of the gap junctional intercellular communication (GJIC) family of proteins.

GJIC is involved in tissue homeostasis and Connexins, a family of gap junction forming proteins, are a key component of GJIC. The Connexin gene family comprises of 21 members in man and 20 in mouse (19 of which can be grouped as orthologous genes) that share high sequence similarity at both gene and protein levels (42); GJA1 (gap junction α-1 or Cx43) is one member of the Connexin family that is highly conserved in mammals (98% protein sequence identity in human and mouse protein sequences) (41). Mutations in Cx43 have been associated with occulo-dentodigital dysplasia (33) and autosomal recessive craniometaphyseal dysplasia (20). Cx43 is the most abundant of the Connexins in skin, and is expressed in keratinocytes, fibroblasts, endothelial cells and dermal appendages (3).

Besides the formation of GJIC, C-terminal portion of Cx43 (CT-Cx43) was reported to localize to the cytosol and nucleus of both cardiomyocytes and HeLa cells(15). Stable expression of CT-Cx43 in HeLa cells induced significant gowth suppression(15). Cx43 plays a role in wound healing during which a decrease in the expression of Cx43 protein is observed within the first 6-48h after injury at the wound edge (3). Topical application of a Cx43-specific antisense oligodeoxynucleotide to acute wounds in rodent models speeds up the wound healing process (27, 36); incidentally, a recent study showed acceleration of wound healing via the activation of the Wnt signaling pathway (54).

Previous work has hinted at a relationship between Wnt signaling, particularly ß-catenin (37) and Cx43 using over-expression or knockdown of Wnt signaling related proteins or Cx43. For example, Cx43 is considered a target of ß-catenin transcription through the activation Wnt signaling with Wnt1 (1, 30, 49); activation of Wnt signaling by Wnt3A, for 72h, also increased expression of Cx43 in vascular smooth muscle cells (9); ß-catenin knockdown reduced Cx43 expression and GJIC in mouse granulosa cells or osteocytes (52, 55). Furthermore, Cx43 overexpression decreased nuclear levels of ß-catenin (46, 47), and reduced TCF luciferase activity in colorectal cancer and neural progenitor cells (37, 39). ß-catenin level increased in conditional osteocytes or sertoli cell knockout Cx43 transgenic mice (6, 7), however, β-catenin expression is attenuated in Cx43 deficient fractures (23). Interestingly, ß-catenin and Cx43 are thought partly to co-localize in the cell membrane (39).

Considering the key functions of Wnt signaling and the putative relationship between ß-catenin, a key transducer of Wnt signaling, and Cx43, we questioned whether Wnt signal activation might modulate Cx43 in mammalian cells? We show here that subsequent to Wnt signaling activation Cx43 is translocated into the nucleus in a similar manner to that of ß-catenin in at least two different mammalian cell lines. ShRNA mediated knockdown of ß-catenin increased intracellular movement of Cx43 to the nucleus and *vice versa*. Quantitation of Cx43 expression shows that the membrane and cytosolic Cx43 is translocated in response to the activation of Wnt signaling and that it interacts with

the proteins associated with the so called ß-catenin destruction complex. We propose that there is cross-talk between Wnt signaling and Cx43 and that Wnt signal activation modulates intracellular Cx43 movement. We provide a new, in vitro, model for the regulation of Cx43 by Wnt signaling and identify a new target protein in response to the activation of Wnt signaling.

## Materials and methods

*Wnt Peptides*

Recombinant Wnts (5A, 9B and 10B) peptides were obtained from (R&D Systems part of Bio-Techne) and were made into stock solutions (at 0.1µg/µl) in phosphate buffered saline (PBS, GIBCO). Cells were treated with Wnts at concentrations described in the figure legends; controls represent untreated or vehicle only treated cells.

*Cell lines*

Cell lines (PC3 human prostate cancer, 3T3 mouse fibroblast) were obtained through ATCC via John Masters (University College London). PC3 cells were grown in RPMI 1640 (Gibco) cell culture medium supplemented with 10% fetal bovine serum (FBS) and L-glutamine. 3T3 fibroblasts were grown in DMEM-GlutaMAX™-1 (Gibco) supplemented with 10% FBS; cells were grown in 5% $CO_2$ at 37°C. Human embryonic kidney (GP-293 and 293FT) cell lines were used for viral transduction and were obtained from the kit manufacturer (Clontech) (25).

*Retroviral and lentiviral constructs and transduction*

Cx43-specific shRNA target sequence GGTGTGGCTGTCAGTGCTC (50) was a gift of W.H. Moolenaar (The Netherlands Cancer Institute); a retroviral pSuper vector (OligoEngine) containing this sequence, designated Cx43shRNA, was used to establish a stable knockdown of Cx43 in cell lines (25); pSuper retroviral vector without Cx43shRNA was used as control. All retroviral vectors were transduced into the packaging cell line GP2–293 (Clontech) as described previously (8).

Lentiviral vectors containing the target sequence for ß-catenin shRNA were obtained from Addgene (MA) and included: pLKO.1 (catalog number, 8453), ß-catenin target (18803) and scramble shRNA (1864). Lentiviral particles were produced in 293FT cells (ATCC, at $7x10^5$) and the transfection complex was prepared using FuGENE 6 Transfection Reagent according to the manufacturer's instructions (Roche). PC3 and 3T3 cells were transduced with retrovirus or lentivirus for 2 days and were selected on the basis of antibiotic resistance.

*Immunocytochemistry*

Immunostaining was performed in two independent laboratories with the experimenter blinded to the identity of the experiments. Cells were grown in eight-well chambered glass slides (Lab Tek II, Nunc) as described, previously (25, 48). The following primary antibodies were used according to the manufacturer's recommendations: Cx43 (catalog number C6219, Sigma) and ß-catenin (ab22656, Abcam). Secondary antibodies (Alexa 488 or 633; Molecular Probes), goat anti-mouse peroxidase Fab (Abcam) and tyramide Cy3 (Perkin Elmer) with Hoechst 33342 or 4',6-diamidino-2-phenylindole (DAPI, Sigma) as a nuclear counterstain were used. Secondary antibody incubation in the absence of primary antibody was used as negative control. A Leica SPE confocal microscope (Leica Microsystems) was used (40x, 1.25 NA objective, sometimes with a zoom of 3x) for imaging; at least three images per well, from 3–5 independent experiments were acquired. Nuclear co-localization of β-catenin was calculated by JACoP analysis in Image J software (38) and represented by Pearson correlation coefficient. Statistical analysis was performed using Mann–Whitney U test.

*Transmission Electron Microscopy (TEM)*

Cells were grown on glass coverslips, treated as previously described (48), and fixed in a mixture of 4% formaldehyde, 0.01% glutaraldehyde in PBS, pH 7.4 for 30mins at $4^oC$. Primary antibodies (Cx43, diluted 1:2000, Sigma or ß-catenin, diluted 1:300) were incubated at $4^oC$ overnight followed by incubation with appropriate secondary antibodies (1.4nm Gold; ab30814 or ab30812 Abcam) also at

142 4°C overnight and post-fixed in 1% glutaraldehyde in phosphate buffer. Post-fixed cells were treated
143 with HQ Silver enhancement kit (Nanoprobes) for 3 min in the dark and then 2% osmium tetraoxide
144 (in the phosphate buffer) for 10min, rinsed, and dehydrated in a series of graded alcohols followed
145 by embedding in Agar 100 resin (Agar Scientific) as an inter-medium. Sections of 80 nm thickness
146 were collected on 300 mesh copper grids and visualised using a Joel 1010 transmission electron
147 microscope (TEM). Images were recorded using a Gatan Orius camera and analyzed using Image J.
148 The levels of Cx43 and β-catenin of different conditions and positions were calculated by setting the
149 same threshold and pixel size. For some types of analysis, images were demarcated into cell
150 membrane, cytosol and nucleus and used to calculate the level of expression of proteins in the
151 demarcated organelle by manually counting the electron dense puncta for analysis. Statistical
152 analysis for significance of difference between two groups was performed using Mann–Whitney U
153 test.
154
155 *Western blotting*
156 PC3 cells (wild type, Cx43shRNA-, pSuper, pLKO.1, scramble shRNA or ß-catenin shRNA transduced)
157 were centrifuged (1500 x*g*) and cell pellets resuspended in ice-cold radioimmunoprecipitation assay
158 buffer (RIPA) buffer with phosphatase and protease inhibitors (Roche). Protein was loaded and
159 separated on a 10% sodium dodecyl sulfate-polyacrylamide gel electrophoresis (SDS-PAGE) and
160 trans-blotted to nitrocellulose membrane (Bio-Rad). The membranes were probed with two
161 different primary antibodies against: Cx43 (C6219, Sigma, diluted 1:4000) and ß-catenin (diluted
162 1:500; ab22656, Abcam). Antibodies against α-tubulin (Sigma) or Glyceraldehyde 3-phosphate
163 dehydrogenase (GAPDH, Sigma) were used as controls for protein quantitation; Horseradish
164 peroxidase (HRP)-conjugated secondary antibodies were used, and proteins were visualized using an
165 enhanced chemiluminescence (ECL) system. Semi-quantitative analysis was performed using ImageJ
166 software and statistical analysis was performed using ANOVA or t-test.
167

*Co-immunoprecipitation*

Cells were lysed using immunoprecipitation buffer (50mM Tris, 150mM NaCl, and 1%NP-40, Sigma) with protease and phosphatase inhibitors to a final volume of 1ml, the lysate was centrifuged (10,000 *x g* for 5 min at 4°C) and protein concentration measured using a BCA assay (Pierce). CK1δ (2-4µg, sc-20709; Santa Cruz Biotechnology) or Cx43 (4µg; C6219, Sigma) antibody was added to 1-2mg total protein and mixed for 1h at 4°C. Protein A agarose (Sigma) was washed with lysis buffer (3x) followed by blocking beads using 1%-2% low-IgG serum for 1h in cold room shaker. Protein A agarose beads (30µl) were added to cell lysate/antibody and mixed O/N, on a rotary shaker, at 4$^{o}$C. The beads were washed 3x in lysis buffer at 4°C and added 50µl 2x loading buffer containing β-mercaptoethanol (10%) to the washed beads to elute the precipitate. Samples were loaded onto a 10% SDS-PAGE gel for electrophoresis to resolve the proteins and Precision Plus Protein™ Dual Color Protein Standards, (Bio Rad) used as molecular weight markers. The resolved protein was transferred onto a nitrocellulose membrane which was cut into strips of 250-75kDa and 70–25kDa as visualized by the markers. The membrane strips were probed with the following antibodies: β-catenin(1:500; ab22656, Abcam), CK1δ(1:200; sc-55553, Santa Cruz Biotechnology, Inc.) and Cx43(1:4000; C8093, Sigma) and then incubated with appropriate secondary antibodies: goat anti-mouse IgG-HRP (1:2000; sc-2005, Santa Cruz Biotechnology) or Goat F(ab')2 Anti-Mouse IgM mu chain-HRP (1:2000; ab5930, Abcam). The signals were detected by ECL detection using ChemiDoc™ XRS+ System with Image Lab™ Software (Bio Rad).

*In vivo rat cutaneous wound-healing model ± Wnts*

All animal procedures were subject to institutional ethical review and performed under the terms of a UK Home Office license. Animals were maintained according to the United Kingdom Home Office Animal (Scientific procedures) Act 1986 Code of Practice and all procedures were approved in a Home Office License. A sample size calculation ($\alpha = 0.05$ and $\beta = 0.05$ and difference of mean of 100) indicated a minimum sample size of 12 animals (8 experimental and 4 control). The animals were

194 housed with 12 hour light – dark cycle with free access to food and water in climatically controlled
195 rooms. Male (8 week old) Sprague-Dawley rats (Harlan Laboratories) were anesthetized by
196 inhalation of 5% halothane and maintained with 1.5% halothane. Their backs were shaved and hair
197 depilatory cream applied, washed with warm water then wiped with 70% ethanol. Skin was then
198 tented and 4 full thickness excision wounds were made with a 6mm diameter punch biopsy (27). A
199 single, topical, application of Wnt5A or Wnt9B (0.2 – 0.5µg/ml) or vehicle control was delivered to
200 each independent wound in 30% Pluronic F-127 gel (Sigma). Wounds were dressed with tegaderm
201 and animals were given analgesic before recovery. They were housed individually before they were
202 humanely killed one or three days after wounding and the wound tissue harvested for further
203 analysis (51, 54). Tissue processing, sectioning and H&E staining were performed as describe before
204 (16). The extent of re-epithelialization was measured and calculated from the wound edge (where
205 the incision was made) to the tip of new growth using Image J. Statistical analysis for significant
206 difference among different groups was performed using ANOVA.
207
208 **Results**
209 *Wnt signaling activates translocation of ß-catenin and Cx43*
210 We previously showed that addition of Wnt ligands (e.g. 5A, 9B) activates the Wnt-signaling pathway
211 as measured by translocation of ß-catenin into the nucleus in PC3 and other mammalian cells (48).
212 Similar results were found in our experiments using immunocytochemistry: there was visible but low
213 expression of ß-catenin (Fig 1 A) in control, vehicle treated, cells. Addition of Wnts increased the
214 expression of ß-catenin in the cytosol and in the nucleus (Fig 1 B-C). We tested the hypothesis that
215 Cx43 may also translocate to the nucleus in response to the activation of Wnt signaling. In PC3 cell
216 line, Cx43 expression was found to be in the cell membrane (Fig 1 D) with punctate staining pattern
217 as has been observed, previously, in other cell types (25). The staining pattern of Cx43 after addition
218 of Wnt5A and 9B (0.2µg/ml), compared to control (vehicle only), PC3 cells, showed Cx43
219 translocation towards the nucleus in a manner similar to that of ß-catenin (Fig 1 E-F). These results

show for the first time that the activation of Wnt signaling results in the intracellular movement of Cx43 towards the nucleus in addition to the established mechanism of translocation of ß-catenin into the nucleus in mammalian cells. Indeed, composite images indicate a level of apparent co-translocation of ß-catenin (red) and Cx43 (green) in Wnt treated PC3 cells (Fig 1) and for Wnt 10B, (Supplemental Fig S1). The Wnt induced translocation of Cx43 was not limited to PC3 cell line only. 3T3 cells treated with Wnt9B showed similar translocation of Cx43 (Supplemental Fig S2) as that observed for PC3 cells. The expression of Cx43 was visible in the nucleus of 3T3 cells after treatment with Wnt9B compared to vehicle control (Supplemental Fig S2). The translocation of Cx43 was also investigated using Western blots in different cell fractions (Supplemental Fig S3). These results confirm the relocation of Cx43 to the nucleus in response to Wnt activation as observed using conventional immunocytochemistry (Fig 1).

*Does the activation of Wnt signaling translocate Cx43 into the nucleus?*

In response to Wnt signaling activation, cytosolic ß-catenin is known to desequester from the 'destruction complex' (44) and translocate into the nucleus where it acts as an activator of transcription factors to increase the expression of genes such as c-Myc, cyclin D1, FRA1 and others (19, 22). Our novel observation that Cx43 also appeared relocated in PC3 cells in response to Wnt signaling (e.g. Fig 1 and Supplemental Fig S3) raised the question whether Cx43, like ß-catenin, also translocates into the nucleus? We used electron microscopy to investigate this, using the same antibodies as those used for immunocytochemistry (Fig 1). The expression of Cx43 was observed on cell membrane and in the cytoplasm in PC3 cells (Fig 2A). It is evident in the electron micrographs that the majority of Cx43 signal appears inside the nucleus subsequent to Wnt signaling activation with Wnt5A or 9B (Fig 2B and 2C). The expression of Cx43 was quantified using Image J from at least 18 micrographs for vehicle control, Wnt5A and Wnt9B treated cells. What was seen by eye was confirmed by quantitation of Cx43 signal in PC3 cells (Fig 2D). We further analyzed the expression of Cx43 in different part of cell (membrane, cytosol and nucleus). Wnt5A or 9B reduced the expression

of Cx43 both on cell membrane and in cytosol (Fig 2 E, F and G); meanwhile both Wnts increased Cx43 expression in the nucleus (Fig 2H). These results indicate, not only that Wnt signaling relocates Cx43 into the cytosol, but also Cx43 translocates to the nucleus in a manner that has previously been shown for ß-catenin (Fig 2I). *Cx43 knockdown: Cx43 and ß-catenin expression*

In order to validate the role of Wnt signaling in translocating Cx43, in addition to its known target, ß-catenin, and to confirm that Cx43 was indeed translocated into the nucleus in response to Wnt activation, we tested the following hypotheses: (i) that down-regulation of Cx43 expression in PC3 cells and other cell lines should eliminate the apparent translocation of Cx43 in response to Wnt signaling (ii) that as with ß-catenin, Cx43 is translocated into the cell nucleus, subsequent to the activation of Wnt signaling.

We tested the above hypotheses by using PC3 cells transduced with a Cx43 short-hairpin RNA (Cx43shRNA) (50) or a control plasmid only (pSuper, termed control). The efficiency of Cx43shRNA knockdown was confirmed by measuring the protein levels of Cx43 by Western blotting; Cx43 protein expression was reduced by 80% in cells transduced with Cx43shRNA compared to control plasmid only transduced cells (Supplemental Fig S4). Cx43shRNA knockdown cells were henceforth termed Cx43kd and the corresponding plasmid only control cells as Cx43c.

We first validated if transduction of control plasmid affected the observed Wnt response for Cx43 and ß-catenin in wild type PC3 cells. Expression of Cx43 and ß-catenin was measured using fluorescence immunocytochemistry as in the wild type cells (as seen in Fig 1, above) with Cx43c cells ± Wnt5A or 9B (Fig 3 A-F). Control experiments demonstrate that plasmid transduction did not alter Wnt mediated Cx43 or ß-catenin response as observed in the wild type cells (Fig 1). Activation of Wnt signaling appeared to relocate intracellular Cx43 protein expression in Cx43c cells and compared to PBS treated cells (Fig 3A) addition of Wnt5A (Fig 3B) or Wnt9B (Fig 3C) appeared to translocate Cx43 protein expression. Furthermore, compared to PBS treated Cx43c cells (Fig 3D),

addition of Wnt ligands (5A and 9B) also induced ß-catenin translocation (Fig 3E and F) as observed in wild type cells. These results also support the notion that Cx43 location is regulated by the Wnt signaling pathway.

Cx43kd cells showed decreased Cx43 expression when measured using immunofluorescence (Fig 3G), this was also the case after Wnt5A or 9B treatment (Fig 3H and I). These results indicate that Cx43 shRNA mediated knockdown reduces the protein expression of Cx43 in Cx43kd cells and supports the data obtained using Western blotting (Supplemental Fig S4).

The expression and distribution of ß-catenin was also determined in Cx43kd cells treated with Wnt ligands using western blot (Supplemental Fig S4) and immunofluorescence (Fig 3 J-L). The total ß-catenin protein levels did not alter significantly after Cx43 knockdown measured using Western blot technique, however, remarkably, the intracellular distribution of ß-catenin was changed (Fig 3J): ß-catenin in the Cx43kd cells appears to be released into the cytosol with limited nuclear co-localization compared to Cx43c cells (Fig 3J compared to Fig 3D and Fig 4A; co-localization of ß-catenin and the nuclear stain, DAPI, was determined using Image J software as described in materials and method). There was a significant increase in the co-localization coefficients of nuclear co-localization of ß-catenin in Cx43kd PC3 cells (Fig 4A). Activation of Wnt signaling by Wnt5A or Wnt9B in Cx43kd cells further increased the nuclear co-localization of ß-catenin compared to these cells with vehicle treatment (Cx43c-vehicle treated < Cx43kd-vehicle treated < Cx43kd Wnt treated, Fig 3K and L and Fig 4A). In addition to the experiments with Cx43kd in PC3 cells (above), similar results were obtained in Cx43kd-3T3 cells (Fig 4B).

These results were validated using electron microscopy (Fig 5) with observations similar to those obtained using immunofluorescence (Fig 3). Compared with vehicle controls (Fig 5A), the nuclear Cx43 expression was increased, significantly, in Cx43c cells treated with Wnts 5A and 9B (Fig 5B-C).

298 The amount of nuclear Cx43 expression was drastically reduced in all groups of Cx43kd cell (Fig 5D-
299 G), whether or not these were treated with Wnts.
300
301 ß-catenin expression was also determined in Cx43kd and Cx43c PC3 cells ± Wnts using TEM (Fig 5H-
302 N); the signal for ß-catenin was increased in Cx43kdshRNA cells relative to Cx43c cells (Fig 5H and K).
303 Subsequent to the activation of Wnt signaling the nuclear expression of ß-catenin was increased
304 significantly ($p$<0.001) in Cx43kd cells (Fig 5L-N) compared to the cells with vehicle treatment (Fig
305 5K). These results indicate that the decrease in the expression of Cx43 leads to ß-catenin
306 displacement in the nucleus without the activation of Wnt signaling and that this process appears to
307 be enhanced after Wnt treatment.
308
309 *ß-Catenin knockdown: Cx43 and ß-catenin expression*
310 To address whether Cx43 distribution was also altered after downregulation of ß-catenin protein we
311 transduced PC3 cells with a ß-catenin short-hairpin RNA (ß-catenin (CTNNB1) shRNA, termed
312 CTNNB1kd) (31) to reduce ß-catenin protein expression; scrambled shRNA (CTNNB1sc) or a plasmid
313 (pLKO.1) only (termed CTNNB1c) transduced cells were used as controls. The efficiency of ß-catenin
314 shRNA knockdown was confirmed by Western blotting. Cells transduced with ß-catenin shRNA
315 showed reduced protein expression (around 80%) compared to CTNNB1sc or CTNNB1c
316 (Supplemental Fig S4). Incidentally, no significant difference was observed in the total Cx43 protein
317 level after CTNNB1 knockdown in Western blots (Supplemental Fig S4).
318
319 Immunofluorescence was used to establish that Wnt response in CTNNB1sc or CTNNB1c was not
320 altered for ß-catenin or Cx43 expression and regulation. Expression of ß-catenin was visible in the
321 nucleus of CTNNB1sc or CTNNB1c cells treated with Wnt5A and Wnt9B compared to the cells that
322 were treated with vehicle control (Fig 6A-C and G-I). The quantified data is given in Fig 4C. Similar
323 results were obtained for Cx43 expression in response to Wnt activation (Fig 6D-F and J-L). These

results indicate that viral transduction did not cause a change in Wnt mediated ß-catenin or Cx43 response as observed in the wild type cells (Fig 1).

CTNNB1kd cells also showed decreased ß-catenin expression using immunofluorescence (Fig 6M), this was also the case even after Wnt treatment (Fig 6N and O). The apparent cellular distribution of Cx43 was different to that observed in CTNNB1c, CTNNB1sc (Fig 6D and J) or wild type cells (Fig 1). There was little Cx43 in the nucleus in CTNNB1c and CTNNB1sc cells (Fig 6D and J), but Cx43 was found in nucleus of CTNNB1kd PC3 cells (Fig 6P); addition of Wnt5A and Wnt9B in CTNNB1kd PC3 cells induced further Cx43 protein to translocate to nucleus compared to vehicle treated cells (Fig 6Q and R).

To further confirm these observations, Cx43 expression was determined in CTNNB1kd cells, CTNNB1c and CTNNB1sc cells in response to Wnts by TEM (Fig 7). Cx43 expression was calculated as expression / nucleus from multiple micrographs. Relative to CTNNB1c and CTNNB1sc cells the nuclear expression of Cx43 was increased in CTNNB1kd cells (Fig 7A, D and G). Also, compared to vehicle treated CTNNB1kd PC3 cells (Fig 7G), cells treated with Wnts 5A or 9B showed an increased nuclear expression of Cx43 (Fig 7H and I). These results indicate that β-catenin knockdown leads to Cx43 translocation to nucleus and this translocation increased in response to Wnt signaling activation.

*Cx43 is a likely partner in the ß-catenin destruction complex*

To examine whether Cx43 was a component of the so called destruction complex (44) we used co-immunoprecipitation technique with β-catenin and CK1 δ (part of the destruction complex proteins), to investigate if Cx43 interacts with the two destruction complex proteins in PC3 cells. We found that both β-catenin and Cx43 were in native CK1δ complexes from PC3 cells (Fig 8). Furthermore, β-catenin and CK1δ were also detected in Cx43 complexes (Fig 8). These results indicate that Cx43,

CK1δ and β-catenin interacts with each other in PC3 cells and Cx43 may be a component of the destruction complex.

*Accelerated re-epithelialization in Wnt ligand-treated wounds in vivo*

A reduction in Cx43 protein expression plays a key role in the wound healing process (3). If Wnt signaling regulates Cx43 *in vitro*, as seen by the experiments described above, can Wnt mediated translocation of Cx43 from *in vivo* wound*s* show similar therapeutic effects on reepithelialisation rates? Having observed that Wnt signal activation accelerates fibroblast cell migration, we next assessed addition of Wnts improved wound healing, *in vivo*, with a gel containing Wnts 5A and 9B, applied to the wound at the time of injury (25). Wnt5A or Wnt9B treatment accelerated the rate of re-epithelialization compared to control rats at 1 day after wounding (Fig 9A-C and G). The significantly increased rate of re-epithelialization, following Wnt5A or 9B treatment, disappeared at 3 days after wounding (Fig 9D-F and G). These results indicated that activation of Wnt signaling has significant effects *in vivo*, similar to those observed for Cx43 knockdown in previous studies (36).

**Discussion**

The mechanism of Wnt signaling has been conventionally thought to be via two distinct pathways the Wnt/ β-Catenin (canonical) and Wnt / $Ca^{2+}$ (non-canonical) (29). In this report, we demonstrate, for the first time, that Wnt signal activation, in addition to the well-established activation of intracellular calcium and translocation of ß-catenin into the nucleus, also leads to the translocation of Cx43 to the nucleus, in mammalian cell lines. Immunostaining, both using fluorescence and TEM, showed Cx43 protein behaves in a similar manner to ß-catenin in response to the activation of Wnt signaling.

Cx43 is best known as a key component of GJIC on the membrane (3, 28) and much research in this field is directed towards understanding the role Cx43 plays in GJIC. For example, in cardiomyocytes and HeLa cells the C-terminal portion of Cx43 (CT-Cx43) is reported to be localized in the cytosol and

nucleus (15). Our results demonstrate that it is the membrane and possibly cytosolic Cx43 that appears, largely, to be translocated into the nucleus subsequent to Wnt signaling activation. These results were validated as the cytosolic/membrane Cx43 signal and its translocation to the nucleus after Wnt activation, were almost completely abolished in cells knocked down for Cx43 in both PC3 and 3T3 cells.

*Nuclear expression of Cx43*

Cx43 contains a nuclear targeting sequence in its C-terminal domain (35, 58) and therefore its presence in the nucleus is not surprising. This occurs for both, the whole, or partial (C-terminus), acetylated or phosphorylated Cx43 protein (10, 11, 13-15, 17, 18, 21, 24, 26, 56, 57). There are other structural clues as to why Cx43 expression is often found in the nucleus. For example, immunoprecipitation and mass spectrometric analysis suggests that Cx43 interacts with two components of the nuclear translocation system: the GTP-binding nuclear protein Ran (RAN) and importin (KPNB1)(18). Furthermore, by using cNLS (nuclear localization signal) Mapper the C-terminal tail of Cx43 has been shown to contain two potential NLSs that are recognized by the importin α/β complex, which imports proteins to the nucleus through the RAN-GTP cycle (18). Also, many Cx43-nuclear interactors have been identified, including several histones, transcription factors and nucleolar proteins, such as nucleolin or the polymerase I and transcript release factor (PTRF). This suggests that Cx43 or its C-terminal tail might affect chromatin organization, nucleolar activity, rRNA transcription and termination (18). During cell cycle progression of A549 lung cancer cell lines, Cx43 is translocated to the nucleus via A-kinase anchoring protein 95 (AKAP95) in late G1 phase. In the nucleus, Cx43-AKAP95 protein complex simultaneously binds DNA and this co-localization implies that Cx43 regulate DNA expression or participate in DNA aggregation and condensation (11). Functionally, nuclear localization of Cx43 has been co-related to slower growth (26), cell cycle progression (11), apoptosis induction (24, 56, 57), activation of gene transcription (13, 18), or tumor formation (14, 17, 21). The extracellular signals that modulate have not been greatly elucidated.

Previous studies have shown that Wnt treatment (with Wnt1 or Wnt3A) for at least 24h or even longer increased the expression of Cx43 and promoted intercellular communication in several cell lines (1, 30, 49). Our investigations demonstrate an effect of Wnt activation on Cx43 in a shorter time span (within minutes), similar to that observed for the documented translocation of Wnt mediated ß-catenin translocation (48).

*Where is Cx43 translocated from in response to Wnt signal activation?*

Estimates from our electron micrographs (Fig 2) show that the range of distribution of Cx43 signal within wild type cells is 10-20%, 20-50% and 5-10% in the cell membrane, cytosol and nucleus, respectively (Fig 2E, F and G). Activation of Wnt signaling results in the re-distribution of Cx43 signal as follows: 5-10%, 10-20% and 50-60% in the cell membrane, cytosol and nucleus, respectively (Fig 2E, F and G). It must be emphasized that these are estimates, based on TEM, and may not reflect the true total distribution of Cx43 within PC3 cells. If, however, the assumptions hold and this is the 'normal' distribution of Cx43 in these cell lines, it would indicate that the majority of Wnt mediated translocation of Cx43 occurs from the cytosolic pool.

*Cx43 expression and ß-catenin, localization and translocation in response to Wnts*

A major extracellular signal for nuclear translocation for Cx43 appears to be extracellular Wnt signal activation. The Wnt signaling pathway is well established as an activator of intracellular ß-catenin translocation into the nucleus. A surprising observation in our study was the apparent relocation of ß-catenin due to Cx43 knockdown (Fig 3J-L, Fig 4 and Fig 5H-N). This observation is complementary to previous studies in which over-expression of Cx43 was reported to show a decrease in the nuclear levels of ß-catenin (46, 47) and reduced TCF luciferase activity in colorectal cancer and neural progenitor cells (37, 39). Conversely, knockdown of β-catenin appears to alter the spatial distribution of Cx43 in PC3 cells. There have been suggestions, sometimes contradictory (6, 7, 23, 52, 55), that

knockdown of either Cx43 or ß-catenin alters the expression of the other. We did not observe alterations in the expression levels of Cx43 or ß-catenin in either PC3 or 3T3 cells that some previous studies suggested (6, 7, 23, 52, 55). This suggests a structural link between intracellular ß-catenin and Cx43 proteins.

Considering that ß-catenin and Cx43 are thought partly to co-localize on the cell membrane (39) and some researchers found that β-catenin appeared to be sequestrated by Cx43 as part of a complex within the junctional membrane (2, 6, 37, 47), these two proteins (ß-catenin and Cx43) may share a closer relationship than expected or reported, previously. Our data add significant weight to this notion, by demonstrating a direct co-relation between the Wnt signaling pathway that regulates the topographical location of ß-catenin and Cx43. These results suggest for the first time, that the two proteins exerting a caging effect upon each other– similar to that of the destruction complex on intracellular ß-catenin (44). And our results indicate that Cx43 may be a component of the destruction complex (Fig 8). The overall impact of ß-catenin and Cx43 appears to be a brake on the displacement of each other under normal conditions whilst moving concomitantly in response to Wnt signal activation.

The results from this study showed that Wnts reduced the expression of Cx43 on the membrane and the cytosol and promoted the translocation of Cx43 into the nucleus. We applied the Wnt5A and 9B ligands to full thickness skin wounds in rats and discovered that Wnt signaling increased the rate of wound healing *in vivo*. As with gene transcription, we observed an impact of Cx43 expression in the migratory capabilities of mammalian cells, *in vitro* (Supplemental Fig S5) *and in vivo* (Fig 9).

We propose a new model (Fig 10) in which activation of Wnt signaling by Wnt ligand / receptor binding activates not only desequestration and translocation of ß-catenin from the destruction

452 complex into the nucleus, as is well known (43), but also release and translocate Cx43 from the
453 membrane and cytosolic compartments into the nucleus.
454
455 **Perspectives and significance**
456 This is the first demonstration of Wnt translocating another protein, other than ß-catenin indicating
457 that Wnt signaling, an evolutionarily conserved signal transduction pathway, may be regulating the
458 topography and the movement of membrane or cytosolic proteins other than the well documented
459 ß-catenin. These results provide a novel mechanism of regulation of a clinically significant
460 cytoskeletal component by a critical cell signaling pathway. This study further demonstrates, for the
461 first time, that Wnt signaling activation translocates Cx43 not just in the cytosol but into the nucleus.
462 Our research provides a novel link between two key areas of cell biology and demonstrates a unique
463 cross talk between these important cell function regulators.
464
465 **Acknowledgements**
466 The authors would like to thank the Prostate Cancer Research Centre, (UK registered charity no.
467 1156027) for financial support. We would also like to thank Michael Millar and Mariana Beltran,
468 University of Edinburgh for help with immunocytochemistry. We are grateful to John Masters,
469 University College London and Tony Davies, University of London for discussions and Jane Pendjiky,
470 University College London for help with Figure 10. We are further thankful to China Scholarship
471 Council for supporting a visiting fellowship for HM.

472 **References**

473 1. **Ai Z, Fischer A, Spray DC, Brown AM, and Fishman GI.** Wnt-1 regulation of connexin43 in
474 cardiac myocytes. *J Clin Invest* 105: 161-171, 2000.
475 2. **Ale-Agha N, Galban S, Sobieroy C, Abdelmohsen K, Gorospe M, Sies H, and Klotz LO.** HuR
476 regulates gap junctional intercellular communication by controlling beta-catenin levels and adherens
477 junction integrity. *Hepatology* 50: 1567-1576, 2009.

3. **Becker DL, Thrasivoulou C, and Phillips AR.** Connexins in wound healing; perspectives in diabetic patients. *Biochim Biophys Acta* 1818: 2068-2075, 2012.

4. **Behrens J, von Kries JP, Kuhl M, Bruhn L, Wedlich D, Grosschedl R, and Birchmeier W.** Functional interaction of beta-catenin with the transcription factor LEF-1. *Nature* 382: 638-642, 1996.

5. **Bhanot P, Brink M, Samos CH, Hsieh JC, Wang Y, Macke JP, Andrew D, Nathans J, and Nusse R.** A new member of the frizzled family from Drosophila functions as a Wingless receptor. *Nature* 382: 225-230, 1996.

6. **Bivi N, Pacheco-Costa R, Brun LR, Murphy TR, Farlow NR, Robling AG, Bellido T, and Plotkin LI.** Absence of Cx43 selectively from osteocytes enhances responsiveness to mechanical force in mice. *J Orthop Res* 31: 1075-1081, 2013.

7. **Carette D, Weider K, Gilleron J, Giese S, Dompierre J, Bergmann M, Brehm R, Denizot JP, Segretain D, and Pointis G.** Major involvement of connexin 43 in seminiferous epithelial junction dynamics and male fertility. *Dev Biol* 346: 54-67, 2010.

8. **Carr AJ and Whitmore D.** Imaging of single light-responsive clock cells reveals fluctuating free-running periods. *Nat Cell Biol* 7: 319-321, 2005.

9. **Carthy JM, Luo Z, and McManus BM.** WNT3A induces a contractile and secretory phenotype in cultured vascular smooth muscle cells that is associated with increased gap junction communication. *Lab Invest* 92: 246-255, 2012.

10. **Chen SC, Pelletier DB, Ao P, and Boynton AL.** Connexin43 reverses the phenotype of transformed cells and alters their expression of cyclin/cyclin-dependent kinases. *Cell growth & differentiation : the molecular biology journal of the American Association for Cancer Research* 6: 681-690, 1995.

11. **Chen X, Kong X, Zhuang W, Teng B, Yu X, Hua S, Wang S, Liang F, Ma D, Zhang S, Zou X, Dai Y, Yang W, and Zhang Y.** Dynamic changes in protein interaction between AKAP95 and Cx43 during cell cycle progression of A549 cells. *Scientific reports* 6: 21224, 2016.

12. **Clevers H and Nusse R.** Wnt/beta-catenin signaling and disease. *Cell* 149: 1192-1205, 2012.

13. **Colussi C, Rosati J, Straino S, Spallotta F, Berni R, Stilli D, Rossi S, Musso E, Macchi E, Mai A, Sbardella G, Castellano S, Chimenti C, Frustaci A, Nebbioso A, Altucci L, Capogrossi MC, and Gaetano C.** Nepsilon-lysine acetylation determines dissociation from GAP junctions and lateralization of connexin 43 in normal and dystrophic heart. *Proc Natl Acad Sci U S A* 108: 2795-2800, 2011.

14. **Crespin S, Fromont G, Wager M, Levillain P, Cronier L, Monvoisin A, Defamie N, and Mesnil M.** Expression of a gap junction protein, connexin43, in a large panel of human gliomas: new insights. *Cancer medicine* 5: 1742-1752, 2016.

15. **Dang X, Doble BW, and Kardami E.** The carboxy-tail of connexin-43 localizes to the nucleus and inhibits cell growth. *Mol Cell Biochem* 242: 35-38, 2003.

16. **Davis NG, Phillips A, and Becker DL.** Connexin dynamics in the privileged wound healing of the buccal mucosa. *WoundRepair Regen* 21: 571-578, 2013.
17. **de Feijter AW, Matesic DF, Ruch RJ, Guan X, Chang CC, and Trosko JE.** Localization and function of the connexin 43 gap-junction protein in normal and various oncogene-expressing rat liver epithelial cells. *Molecular carcinogenesis* 16: 203-212, 1996.
18. **Gago-Fuentes R, Fernandez-Puente P, Megias D, Carpintero-Fernandez P, Mateos J, Acea B, Fonseca E, Blanco FJ, and Mayan MD.** Proteomic Analysis of Connexin 43 Reveals Novel Interactors Related to Osteoarthritis. *Molecular & cellular proteomics : MCP* 14: 1831-1845, 2015.
19. **Heo JS, Lee SY, and Lee JC.** Wnt/beta-catenin signaling enhances osteoblastogenic differentiation from human periodontal ligament fibroblasts. *Mol Cells* 30: 449-454, 2010.
20. **Hu Y, Chen IP, de AS, Tiziani V, Do Amaral CM, Gowrishankar K, Passos-Bueno MR, and Reichenberger EJ.** A novel autosomal recessive GJA1 missense mutation linked to Craniometaphyseal dysplasia. *PLoSOne* 8: e73576, 2013.
21. **Huang RP, Fan Y, Hossain MZ, Peng A, Zeng ZL, and Boynton AL.** Reversion of the neoplastic phenotype of human glioblastoma cells by connexin 43 (cx43). *Cancer Res* 58: 5089-5096, 1998.
22. **Huelsken J and Behrens J.** The Wnt signalling pathway. *JCell Sci* 115: 3977-3978, 2002.
23. **Loiselle AE, Lloyd SA, Paul EM, Lewis GS, and Donahue HJ.** Inhibition of GSK-3beta rescues the impairments in bone formation and mechanical properties associated with fracture healing in osteoblast selective connexin 43 deficient mice. *PLoS ONE* 8: e81399, 2013.
24. **Mauro V, Carette D, Pontier-Bres R, Dompierre J, Czerucka D, Segretain D, Gilleron J, and Pointis G.** The anti-mitotic drug griseofulvin induces apoptosis of human germ cell tumor cells through a connexin 43-dependent molecular mechanism. *Apoptosis : an international journal on programmed cell death* 18: 480-491, 2013.
25. **Mendoza-Naranjo A, Cormie P, Serrano AE, Hu R, O'Neill S, Wang CM, Thrasivoulou C, Power KT, White A, Serena T, Phillips AR, and Becker DL.** Targeting Cx43 and N-cadherin, which are abnormally upregulated in venous leg ulcers, influences migration, adhesion and activation of Rho GTPases. *PLoS ONE* 7: e37374, 2012.
26. **Mennecier G, Derangeon M, Coronas V, Herve JC, and Mesnil M.** Aberrant expression and localization of connexin43 and connexin30 in a rat glioma cell line. *Molecular carcinogenesis* 47: 391-401, 2008.
27. **Mori R, Power KT, Wang CM, Martin P, and Becker DL.** Acute downregulation of connexin43 at wound sites leads to a reduced inflammatory response, enhanced keratinocyte proliferation and wound fibroblast migration. *J Cell Sci* 119: 5193-5203, 2006.
28. **Nielsen MS, Axelsen LN, Sorgen PL, Verma V, Delmar M, and Holstein-Rathlou NH.** Gap junctions. *Compr Physiol* 2: 1981-2035, 2012.
29. **Nusse R.** Wnt signaling. *Cold Spring HarbPerspectBiol* 4: pii: a011163, 2012.
30. **Olson DJ, Christian JL, and Moon RT.** Effect of wnt-1 and related proteins on gap junctional communication in Xenopus embryos. *Science* 252: 1173-1176, 1991.

31. **Onder TT, Gupta PB, Mani SA, Yang J, Lander ES, and Weinberg RA.** Loss of E-cadherin promotes metastasis via multiple downstream transcriptional pathways. *Cancer Res* 68: 3645-3654, 2008.

32. **Ozawa M, Baribault H, and Kemler R.** The cytoplasmic domain of the cell adhesion molecule uvomorulin associates with three independent proteins structurally related in different species. *EMBO J* 8: 1711-1717, 1989.

33. **Paznekas WA, Boyadjiev SA, Shapiro RE, Daniels O, Wollnik B, Keegan CE, Innis JW, Dinulos MB, Christian C, Hannibal MC, and Jabs EW.** Connexin 43 (GJA1) mutations cause the pleiotropic phenotype of oculodentodigital dysplasia. *AmJHumGenet* 72: 408-418, 2003.

34. **Peifer M, McCrea PD, Green KJ, Wieschaus E, and Gumbiner BM.** The vertebrate adhesive junction proteins beta-catenin and plakoglobin and the Drosophila segment polarity gene armadillo form a multigene family with similar properties. *J Cell Biol* 118: 681-691, 1992.

35. **Qin H, Shao Q, Curtis H, Galipeau J, Belliveau DJ, Wang T, Alaoui-Jamali MA, and Laird DW.** Retroviral delivery of connexin genes to human breast tumor cells inhibits in vivo tumor growth by a mechanism that is independent of significant gap junctional intercellular communication. *J Biol Chem* 277: 29132-29138, 2002.

36. **Qiu C, Coutinho P, Frank S, Franke S, Law LY, Martin P, Green CR, and Becker DL.** Targeting connexin43 expression accelerates the rate of wound repair. *Curr Biol* 13: 1697-1703, 2003.

37. **Rinaldi F, Hartfield EM, Crompton LA, Badger JL, Glover CP, Kelly CM, Rosser AE, Uney JB, and Caldwell MA.** Cross-regulation of Connexin43 and beta-catenin influences differentiation of human neural progenitor cells. *Cell Death Dis* 5: e1017, 2014.

38. **Schindelin J, Arganda-Carreras I, Frise E, Kaynig V, Longair M, Pietzsch T, Preibisch S, Rueden C, Saalfeld S, Schmid B, Tinevez JY, White DJ, Hartenstein V, Eliceiri K, Tomancak P, and Cardona A.** Fiji: an open-source platform for biological-image analysis. *NatMethods* 9: 676-682, 2012.

39. **Sirnes S, Bruun J, Kolberg M, Kjenseth A, Lind GE, Svindland A, Brech A, Nesbakken A, Lothe RA, Leithe E, and Rivedal E.** Connexin43 acts as a colorectal cancer tumor suppressor and predicts disease outcome. *Int J Cancer* 131: 570-581, 2012.

40. **Slusarski DC, Yang-Snyder J, Busa WB, and Moon RT.** Modulation of embryonic intracellular Ca2+ signaling by Wnt-5A. *DevBiol* 182: 114-120, 1997.

41. **Sohl G and Willecke K.** Gap junctions and the connexin protein family. *CardiovascRes* 62: 228-232, 2004.

42. **Sohl G and Willecke K.** An update on connexin genes and their nomenclature in mouse and man. *Cell CommunAdhes* 10: 173-180, 2003.

43. **Stamos JL and Weis WI.** The beta-catenin destruction complex. *Cold Spring HarbPerspectBiol* 5: a007898, 2013.

44. **Suh EK and Gumbiner BM.** Translocation of beta-catenin into the nucleus independent of interactions with FG-rich nucleoporins. *ExpCell Res* 290: 447-456, 2003.

45. **Sutcliffe JE, Chin KY, Thrasivoulou C, Serena TE, O'Neil S, Hu R, White AM, Madden L, Richards T, Phillips AR, and Becker DL.** Abnormal connexin expression in human chronic wounds. *The British journal of dermatology* 173: 1205-1215, 2015.

46. **Talhouk RS, Fares MB, Rahme GJ, Hariri HH, Rayess T, Dbouk HA, Bazzoun D, Al-Labban D, and El-Sabban ME.** Context dependent reversion of tumor phenotype by connexin-43 expression in MDA-MB231 cells and MCF-7 cells: role of beta-catenin/connexin43 association. *Exp Cell Res* 319: 3065-3080, 2013.

47. **Talhouk RS, Mroue R, Mokalled M, Abi-Mosleh L, Nehme R, Ismail A, Khalil A, Zaatari M, and El-Sabban ME.** Heterocellular interaction enhances recruitment of alpha and beta-catenins and ZO-2 into functional gap-junction complexes and induces gap junction-dependant differentiation of mammary epithelial cells. *Exp Cell Res* 314: 3275-3291, 2008.

48. **Thrasivoulou C, Millar M, and Ahmed A.** Activation of intracellular calcium by multiple Wnt ligands and translocation of beta-catenin into the nucleus: a convergent model of Wnt/Ca2+ and Wnt/beta-catenin pathways. *J Biol Chem* 288: 35651-35659, 2013.

49. **van der Heyden MA, Rook MB, Hermans MM, Rijksen G, Boonstra J, Defize LH, and Destree OH.** Identification of connexin43 as a functional target for Wnt signalling. *J Cell Sci* 111 ( Pt 12): 1741-1749, 1998.

50. **van Zeijl L, Ponsioen B, Giepmans BN, Ariaens A, Postma FR, Varnai P, Balla T, Divecha N, Jalink K, and Moolenaar WH.** Regulation of connexin43 gap junctional communication by phosphatidylinositol 4,5-bisphosphate. *J Cell Biol* 177: 881-891, 2007.

51. **Wang CM, Lincoln J, Cook JE, and Becker DL.** Abnormal connexin expression underlies delayed wound healing in diabetic skin. *Diabetes* 56: 2809-2817, 2007.

52. **Wang HX, Gillio-Meina C, Chen S, Gong XQ, Li TY, Bai D, and Kidder GM.** The canonical WNT2 pathway and FSH interact to regulate gap junction assembly in mouse granulosa cells. *Biol Reprod* 89: 39, 2013.

53. **Wang Q, Symes AJ, Kane CA, Freeman A, Nariculam J, Munson P, Thrasivoulou C, Masters JR, and Ahmed A.** A novel role for wnt/ca signaling in actin cytoskeleton remodeling and cell motility in prostate cancer. *PLoS ONE* 5: e10456, 2010.

54. **Whyte JL, Smith AA, Liu B, Manzano WR, Evans ND, Dhamdhere GR, Fang MY, Chang HY, Oro AE, and Helms JA.** Augmenting endogenous Wnt signaling improves skin wound healing. *PLoSOne* 8: e76883, 2013.

55. **Xia X, Batra N, Shi Q, Bonewald LF, Sprague E, and Jiang JX.** Prostaglandin promotion of osteocyte gap junction function through transcriptional regulation of connexin 43 by glycogen synthase kinase 3/beta-catenin signaling. *Mol Cell Biol* 30: 206-219, 2010.

56. **Xie H, Cui Y, Hou S, Wang J, Miao J, Deng F, and Feng J.** Evaluation of Connexin 43 Redistribution and Endocytosis in Astrocytes Subjected to Ischemia/Reperfusion or Oxygen-Glucose Deprivation and Reoxygenation. *BioMed research international* 2017: 5064683, 2017.

57. **Zhao X, Tang X, Ma T, Ding M, Bian L, Chen D, Li Y, Wang L, Zhuang Y, Xie M, and Yang D.** Levonorgestrel Inhibits Human Endometrial Cell Proliferation through the Upregulation of Gap Junctional Intercellular Communication via the Nuclear Translocation of Ser255 Phosphorylated Cx43. *BioMed research international* 2015: 758684, 2015.

58. **Zhou JZ and Jiang JX.** Gap junction and hemichannel-independent actions of connexins on cell and tissue functions--an update. *FEBS letters* 588: 1186-1192, 2014.

**Figure Legends**

Figure1

Translocation of β-catenin (red) and Cx43 (green) to the nucleus (counterstained with DAPI, blue) in response to activation by Wnt ligands (200ng/ml) in PC3 cell line using immunocytochemistry. Control vehicle treated (A, D) or after activation with Wnt5A (B, E) and Wnt9B (C, F). *Inset*: shows the larger field from which the higher magnification images were taken. Z-stacks were obtained using a Leica SPE confocal microscope. Wnt activation increases the translocation of both ß-catenin (red) and Cx43 (green) translocation towards the nucleus. Representative images of three individual experiments are shown. Scale bar= 10µm.

Figure 2

Translocation of Cx43 to the nucleus in response to Wnt ligands (200ng/ml) in PC3 cell line, control (A) or after activation with Wnt5A (B) and Wnt9B (C). PC3 cells were grown on coverslips, treated with Wnt ligands, fixed, and stained for Cx43 EM investigation. Representative images obtained using a TEM microscope are shown; white dotted lines demarcate the nuclear boundary; white arrows indicate some of the Cx43 labelled electron dense puncta; purple arrows indicate putative Cx43 hemi-channels. *Inset*: High-magnification images of the nuclear region. Scale bar, 2µm. Between 18–25 cells were analyzed and box plots show calculated Cx43 level/nucleus (D); there was a significant (***$p$<0.0001) increase in the Cx43 signal in the nuclei of cells treated with Wnt (5A, box shaded green and 9B, box shaded blue) compared to vehicle control (box shaded yellow). The distribution of calculated Cx43 expression (data binned) on the cell membrane (green), in the cytosol

(red) and nucleus (purple) separately in response to activation by Wnt ligands (200ng/ml) in PC3 cells (E-G). Cells were analyzed from EM images of control (E) or after activation with Wnt5A (F) and Wnt9B (G) were analyzed as described under "Experimental Procedures." Activation of Wnt signaling results in the re-distribution of Cx43 signal as follows: 5-10, 10-20 and 50-60 in the cell membrane, cytosol and nucleus, respectively. Box plot of calculated Cx43 (H) and β-catenin (I) expression, represented by mean count of electron dense puncta, on the cell membrane (box border: blue/green), in the cytosol (box border: pink) and nucleus (box border: purple) in untreated controls (box fill: orange) and in response to activation by Wnt (200ng/ml) 5A (box fill: green) and 9B (box fill: blue) in PC3 prostate cancer cell line. Images were obtained using a TEM microscope similar to those used in e.g. Figs 2 and 7. Cx43 (H) expression was reduced in the membrane and cytosol, increased in nucleus, significantly for Wnt-treated compared to control cells. The expression of β-catenin (I) in cytosol and nucleus increased significantly for Wnt-treated versus control cells; 25 cells from 3 independent experiments were analyzed. Mann-Whitney U test was used to measure the significance of difference between control and Wnt treated cells is annotated (ns = not significantly different; *$p$<0.05; **$p$<0.01;***$p$<0.0001).

Figure 3

Cx43 and β-catenin translocation to the nucleus in response to activation by Wnt ligands (200ng/ml) in Cx43c PC3 prostate cancer cell lines, control (A, D) or after activation with Wnt5A (B, E) and Wnt9B (C, F); Cx43 expression was decreased in Cx43kd cells, control (G) or after Wnt5A (H) or 9B treatment (I), as would be expected, and more β-catenin translocation were observed in Cx43kd cells, control (J) or after activation with Wnt5A (K) and Wnt9B (L). Cells were grown in eight-well chamber slides, treated with Wnt ligands, fixed, and stained for β-catenin (red), Cx43 (green) and nucleus (blue). Representative images from three independent experiments are shown as Z-stacks obtained using a Leica SPE confocal microscope. Scale bar, 10μm.

Figure 4

Co-localization of ß-catenin or Cx43 with DAPI (nuclear counterstain) in wild type and knock-down cells

(A) Box plots of calculated Pearson coefficient for β-catenin co-localization in the nucleus in Cx43c and Cx43kd PC3 cells. Immunohistochemistry and image analysis was performed as described under "Experimental Procedures". Cy3 (label for β-catenin) showed significantly increased co-localization coefficients with DAPI (nuclear counterstain) for Wnt-treated (200 ng/ml) versus control cells in both Cx43c and Cx43kd cells (at least *$p$<0.05). Co-localization coefficients of β-catenin was significantly increased in Cx43kd cells compared with Cx43c cells ( § $p$<0.0002) and between vehicle treated controls and Wnt (5A or 9B) treated cells (asterisks, *$p$<0.05*** $p$ <0.001) within Cx43c (hollow bars) and Cx43kd cells (shaded bars), respectively (n= 49-106 cells for each condition from 2-3 independent experiments).

(B) Box plots of calculated Pearson coefficient for β-catenin co-localization in the nucleus in Cx43c and Cx43kd 3T3 cells. Immunohistochemistry and image analysis was performed as described under "Experimental Procedures". Cy3 (label for β-catenin) showed significantly increased co-localization coefficients with DAPI (nuclear counterstain) for Wnt-treated (200 ng/ml) versus control cells in both Cx43c and Cx43kd cells ($p$<0.05). Co-localization coefficients of β-catenin was significantly increased in Cx43kd cells compared with Cx43c cells ( § $p$<0.02) and between vehicle treated controls and Wnt (5A or 9B) treated cells (asterisks *$p$ <0.05 and ** $p$ <0.01) within Cx43c (hollow bars) and Cx43kd cells (shaded bars), respectively (n = 32-172 cells from 2-3 independent experiments).

(C) Box plots for the calculated Pearson co-localization coefficient of β-catenin and nuclear counterstain DAPI indicating ß-catenin translocation into the nucleus in CTNNB1c (wild type, hollow bars), CTNNB1sc (scramble shRNA control, hatched bars) and CTNNB1kd (Cx43 knockdown, shaded bars) PC3 cells. Immunohistochemistry and image analysis was performed as described under

704 ”Experimental Procedures” and between 16-144 cells for each conditions from 2-3 independent
705 experiments were analyzed. There was no significant difference in the co-localization coefficients of
706 ß-catenin between control, CTNNB1c (hollow gray bar) and CTNNB1sc (hatched gray bar). Co-
707 localization coefficient for β-catenin was significantly (asterisks *$p$<0.05, *** $p$<0.001) increased in
708 Wnt treated CTNNB1c (hollow, 5A green, 9B blue) and CTNNB1sc (hatched, 5A green, 9B blue),
709 compared to their respective control, vehicle treated, cells.

710 Figure 5

711 TEM of Cx43 and β-catenin translocation to the nucleus in response to activation by Wnt ligands
712 (200ng/ml) in Cx43c (vector only control) and Cx43kd (shRNA knockdown) PC3 cells. Cx43 protein
713 expression was measured in vehicle only (A,D) or after activation with Wnt5A (B,E) and Wnt9B (C,F)
714 in Cx43c and Cx43kd cells, respectively. There was a significant increase in puncta/nucleus in Wnt
715 treated Cx43c cells compared to vehicle controls (**, $p$<0.001). There was no statistically significant
716 difference in the Cx43 positive puncta/nucleus between vehicle treated or Wnt treated Cx43kd cells
717 (G). Similar to fluorescence immunohistochemistry results, there was a significant increase in the
718 translocation of ß-catenin protein into the nucleus in Wnt treated cells (I,J) compared to vehicle
719 control (H) Cx43c cells using TEM. Measurement of the expression of ß-catenin protein (N) also
720 showed that significantly (section, § $p$<0.001) more β-catenin-positive puncta were translocated to
721 the nucleus in Cx43kd cells (K), compared to Cx43c cells (H); There was also a significant (star ★
722 $p$<0.001) increase in ß-catenin expression in Wnt5A treated compared to vehicle control in Cx43kd
723 cells (L); there was no significant difference in vehicle control vs Wnt 9B treated Cx43kd cells (M). A
724 quantitation of ß-catenin protein expression in Cx43c and Cx43kd cells is given in (N). *Inset*: shows
725 the larger field from which the higher magnification images were taken. Scale bar, 2µm. EM image
726 analysis was performed as described under “Experimental Procedures.” Between 17-38 cells from 3
727 independent experiments were analyzed and box plots show calculated number of electron dense
728 puncta of Cx43 (G) or β-catenin (N) per nucleus.

729 Figure 6

730 Immunocytochemical analysis of β-catenin (red) and Cx43 (green) translocation to the nucleus (blue)
731 in response to activation by Wnt ligands (200ng/ml) in CTNNB1c and CTNNB1sc PC3 prostate cancer
732 cell line, vehicle control (A, D,G, J) or after activation with Wnt5A (B,E,H,K) and Wnt9B (C,F,I,L); more
733 Cx43 translocation was observed in CTNNB1kd cells, control (P) or after activation with Wnt5A (Q)
734 and Wnt9B (R). ß-catenin expression was decreased in CTNNB1kd cells (M), this was also the case
735 even after Wnt treatment (N and O). Cells were grown in eight-well chamber slides, treated with
736 Wnt ligands, fixed, and stained for β-catenin, Cx43 and nucleus using immunocytochemistry
737 protocols described under "Experimental Procedures". Z-stacks obtained using a Leica SPE confocal
738 microscope are shown. Representative images of three individual experiments are shown. Scale bar
739 = 10μm.

740 Figure 7

741 Translocation of Cx43 to the nucleus in response to activation by Wnt ligands (200ng/ml) in
742 CTNNB1c and CTNNB1sc PC3 cells line using TEM. Vehicle treated, control (A, D) or after activation
743 with Wnt5A (B, E) and Wnt9B (C, F). Increased Cx43 translocation was observed in CTNNB1kd cells,
744 control (G) or after activation with Wnt5A (H) and Wnt9B (I) compared to Wnt treated CTNNB1c and
745 CTNNB1sc. Between 20-76 cells from 2-3 independent experiments were analyzed. Representative
746 images of three individual experiments are shown. Scale bar = 2μm.

747

748 Figure 8

749 β-catenin, Cx43 and CK1δ interact with each other in PC3 cells. (A) Immunoblot/co-IP analysis of the
750 native CK1δ complex from whole-cell PC3 lysates using antibody indicated at the left of each panel.
751 Both β-catenin and Cx43 were detected in native CK1δ complexes from PC3 cells. (B)
752 Immunoblot/co-IP analysis of the native Cx43 complex from whole-cell PC3 lysates using antibody
753 indicated at the left of each panel. Both β-catenin and CK1δ were detected in Cx43 complexes from

PC3 cells. The IP antibodies were used with CK1δ (4µg; sc-20709; Santa Cruz Biotechnology) and Cx43 (4ug; C6219, Sigma). The primary antibodies for Western blot were used with β-catenin (1:500; ab22656, Abcam), CK1δ (1:200; sc-55553, Santa Cruz Biotechnology) and Cx43 (1:4000; C8093, Sigma). The secondary antibodies were used with goat anti-mouse IgG-HRP (1:2000; sc-2005, Santa Cruz Biotechnology) and Goat F(ab')2 Anti-Mouse IgM mu chain-HRP (1:2000; ab5930, Abcam). Lanes are numbered 1, 2 and 3 for input, CKIδ and IgG, respectively; MW indicates the molecular weight marker lane. A representative of 3 independent experiments is shown.

Figure 9

Re-epithelialization rates (straight-line measurement from wound edge to distal tongue of re-epithelization into the wound-bed) following injury in control and Wnts treated rat skin epidermis. Images show examples of re-epithelialization in rat skin epidermis rates at 1 day post-wounding (dpw), control (A), Wnt5A (B), and Wnt9B (C) treated; and at 3 day post-wounding, control (D), Wnt5A (E), and Wnt9B (F) treated. White dotted lines indicate the dermal-epidermal border of re-epithelialization. (G) Box plot (shaded yellow for vehicle control, green for Wnt5A and blue for Wnt9B treated animals; n=8 for Wnt treated rats and n=5 for control at 1 and 3 dpw) showing the rate of re-epithelialization was significantly (** $p<0.02$) increased relative to controls in Wnt treated rats at 1 day post-wounding (dpw, brown outlined box). The rate of re-epithelialization was similar relative to controls in Wnt treated rats at 3 day post-wounding (gray outlined box).

Figure 10

A model for Wnt signaling pathway that regulates ß-catenin and Cx43 in mammalian cell lines (only the cell membrane and the nucleus shown in the schematic for clarity). Proposed steps of Wnt signaling in mammalian cells are as follows: binding of Wnts (1) results in the activation of intracellular calcium stores (2) that increase in the intracellular concentration of free calcium (3). The increase in free calcium depolarizes the cell membrane and as calcium enters the nucleus (4), the nuclear envelope (NE) is depolarized (48); the activation of Wnt/Ca2+ pathway also increases (5)

780 Ca2+/calmodulin-dependent kinase (CamKII) activity (53). It is well established by previous studies
781 (29) (that activation of Wnt signaling (6) desequesters the caged β-catenin (β-cat) that is
782 phosphorylated (P) and ubiquitinated (UUU) prior to degradation in proteasomes, gray square) in
783 the cytosol. The desequestered β-catenin (7) translocation is facilitated across the NE, which is now
784 depolarized (8) and has increased nucleoplasmic calcium (9). Cx43 and β-catenin are partly
785 colocalized at the cell membrane (39). Cx43 is a likely partner in the ß-catenin destruction complex.
786 The membrane and cytosolic Cx43 are moving with ß-catenin concomitantly and largely translocated
787 into the nucleus subsequent to Wnts signaling activation. β-catenin and Cx43 are co-localized in the
788 nucleus where β-catenin binds to LEF/TCF proteins to initiate gene transcription and Cx43 is a likely
789 co-transcription factor. For simplification, many other proteins involved in Wnt signaling are not
790 shown and multiple other pathways such as Wnt/PCP pathways are not included in the illustration.
791 The steps for which evidence is given in the manuscript are shown with arrows shaded purple.
792

Supplemental Figure 1

Confocal images of simultaneous detection of ß-catenin and Cx43 translocation to the nucleus in response to activation by Wnt 10B in PC3 prostate cancer cell line. Cells were grown in eight-well chamber slides and wells were either treated with Wnt 10B (200ng/ml) or with PBS (control) – manual staining was performed using primary (see methods) and appropriate secondary fluorophore labelled antibodies. A to D are individual channels for (A) DAPI, nuclear stain (blue), (B) Cx43 (green) and (C)ß-catenin (red); D is a composite image of all the channels. Images E to H are for Wnt 10B treated cells; individual channels for (E) DAPI, nuclear stain (blue), (f) Cx43 (green) and (G)ß-catenin (red); H is a composite image of all the channels. Individual Z-stacks were obtained using a Leica SPE confocal microscope are shown. Representative images of three individual experiments are shown. Scale bar = 10µm.

Supplemental Figure S2

Confocal images of Cx43 translocation to the nucleus in response to activation by Wnt ligands (200ng/ml) in 3T3 fibroblast cell line, in control (A) and Wnt 9B treated cells (B). Cells were grown in eight-well chamber slides, treated with Wnt ligands, fixed, and stained for Cx43 (green) and nucleus (counterstained with DAPI, blue) using protocols described under “Experimental Procedures.” Z-stacks obtained using a Leica SPE confocal microscope are shown. Representative images of three individual experiments are shown. Scale bar = 10µm.

Supplemental Figure S3

A representative Western blot (n=3) from two independent cell fractionation experiments of PC3 cells with and without (A) Wnt 5A and (B) Wnt 9B treatment. Each lane of the gel was loaded with 12 µg of fractionated protein (untreated and treated, respectively – see methods below): cytosolic (Cytosol, lanes 2 and 3), cell membrane (Cell Memb., lanes 5 and 6) and nuclear (Nuclear, lanes 8 and 9); lanes 1, 4, 7 and 10 were loaded with Precision Plus Protein Dual Color Standards (Bio Rad).

The PVDF membranes were cut into two strips of 250 to 50 kDa and 50 to 10 kDa and incubated with anti-Lamin A (expected size ~70k Da), a marker for the nuclear fraction, and anti-Cx43 (expected size ~41-43k Da) antibodies (both shown in black boxes), respectively. The 50 to 10kDa blot was 'stripped' (shown in a blue box) and further probed with ß-actin (expected size ~42k Da).

Cell fractionation was performed using Qproteome cell compartment kit (Qiagen) according to manufacturer's protocol. Briefly, PC3 cells were grown in 25ml flasks and treated with Wnt5A and Wnt9B in PBS (1.5ml) at 37$^{o}$C as described in methods; vehicle treated PC3 cells were used as controls. The cell were lysed and fractionated into cytosolic (Cytosol), cell membrane (Cell Memb.) and nuclear (Nuclear) fractions using the Qproteome (Qiagen) followed by protein quantitation using Pierce BCA protein assay kit (Thermo Fisher Scientific); 12 µg protein for each fraction was loaded onto gels and resolved on Precast Gels (Bio Rad)using Mini-PROTEAN (Bio Rad) system. The resolved proteins were transferred onto a PVDF membrane using Trans-Blot® TurboTM Blotting System (Bio Rad). The PVDF membranes were cut into two strips of 250 to 50 kDa and 50 to 10 kDa and incubated with anti-Lamin A (cat no. L1238, Sigma, at 1:5000 dilution), a marker for the nuclear fraction, and anti-Cx43 (C6219, Sigma, at 1:8000 dilution, expected size ~41-43k Da) antibodies, respectively for over-night at 4°C. Following this, the PVDF membranes were washed and probed with appropriate Horse Radish Peroxidase (HRP) conjugated secondary antibodies (Peroxidase AffiniPure Donkey Anti-Rabbit IgG (H+L), dilution 1:10000, Jackson ImmunoResearch Laboratories, Inc) for 120 min at RT. The HRP signal was detected using Bio Rad Clarity Western Enhanced Chemi-luminescence (ECL) substrate and blots were imaged using Chemi Doc (Bio Rad) system. Dual colored standard protein markers (Bio Rad Precision Plus Protein, Bio Rad) were used which are recognized by the Chemi Doc system. ß-actin, a 42 kDa ubiquitous protein, a commonly used as a protein loading control was also used. To detect ß-actin the 50 to 10 kDa PVDF membrane strip (see above) was 'stripped' using Thermo Scientific Restore PLUS Western Blot Stripping Buffer (Ref: 46430) using standard protocols and incubated with anti-ß-actin antibody (ab6276, Abcam, at 1:5000 dilution, expected size ~42k Da). Subsequent to detection with an HRP secondary antibody (Peroxidase AffiniPure Donkey Anti-Mouse IgG (H+L), Jackson ImmunoResearch Laboratories, Inc), the HRP signal was detected as described earlier.

Supplemental Figure S4

847 Western blots to confirm knockdown of Cx43 and ß-catenin using Tubulin (Tub) was included as
848 loading control.

849 (A) Cx43 expression in control and Cx43 knockdown cells measured by Western blotting in Cx43c and
850 Cx43kd in PC3 cells (representative blots on top and quantified data underneath). Cx43 level was
851 significantly reduced in Cx43kd cells compared with Cx43c cells. Quantitation of the signal shows
852 that Cx43 protein levels were knocked down in Cx43kd PC3 cells compared to Cx43c cells (* $p<0.05$;
853 n = 3).

854 (B) ß-catenin expression in control and Cx43 knockdown cells measured by Western blotting.
855 Knockdown of Cx43 did not change the expression levels of β-catenin in PC3 cells. β-catenin levels
856 were analyzed by Western blot in Cx43c and Cx43kd PC3 prostate cancer cell lines. Quantitation of
857 the signal shows that knockdown of Cx43 did not change the expression levels of β-catenin.

858 (C) Anti-β-catenin antibody on PC3 cells; vector only control (CTNNB1c), scrambled shRNA control
859 (CTNNB1sc) and short-hairpin RNA to knockdown ß-catenin expression (CTNNB1kd). ß-catenin levels
860 were significantly reduced in CTNNB1kd PC3 cells compared with CTNNB1c and CTNNB1sc cells.
861 Quantitation of the signal shows that β-catenin knockdown in CTNNB1kd PC3 cells compared to
862 CTNNB1c and CTNNB1sc cells (* indicates significant change in expression compared to control,
863 $p<0.05$; n = 3).

864 (D) Knockdown of β-catenin did not change the expression levels of Cx43 in PC3 cells using Western
865 blotting. Cx43 levels were measured in CTNNB1c, CTNNB1sc and CTNNB1kd PC3 prostate cancer cell
866 line. Quantitation of the signal shows that knockdown of β-catenin did not change the expression
867 levels of Cx43.

868

869 Supplemental Figure S5

870 Box plots of the rate of wound closure, in Cx43c (vector only, gray outlined box) and Cx43kd (Cx43
871 knockdown, brown outlined box) 3T3 fibroblast cells. Cells were wounded using WoundMaker
872 (Essen) and imaged for 48h at 2h interval. Cx43 knockdown accelerated the rate of cell migration
873 compared with Cx43c control cells (yellow shaded box, § $p<0.001$). Addition of Wnt5A (shaded
874 green) and Wnt 9B (shaded blue) accelerated the rate of wound closure in Cx43c cells compared to
875 vehicle treated controls (asterisks, **$p<0.01$;***$p<0.001$) but did not impact (ns, not significant)
876 upon the rate of wound closure in Cx43kd vehicle treated control cells compared to the respective
877 Wnt treated cells. Significance of difference between conditions was measured using the Mann
878 Whitney U test.

879 Supplemental data can be accessed at: https://figshare.com/s/1e0dcade1c40ab536ce9

880

881

882

883

884

Fig 1

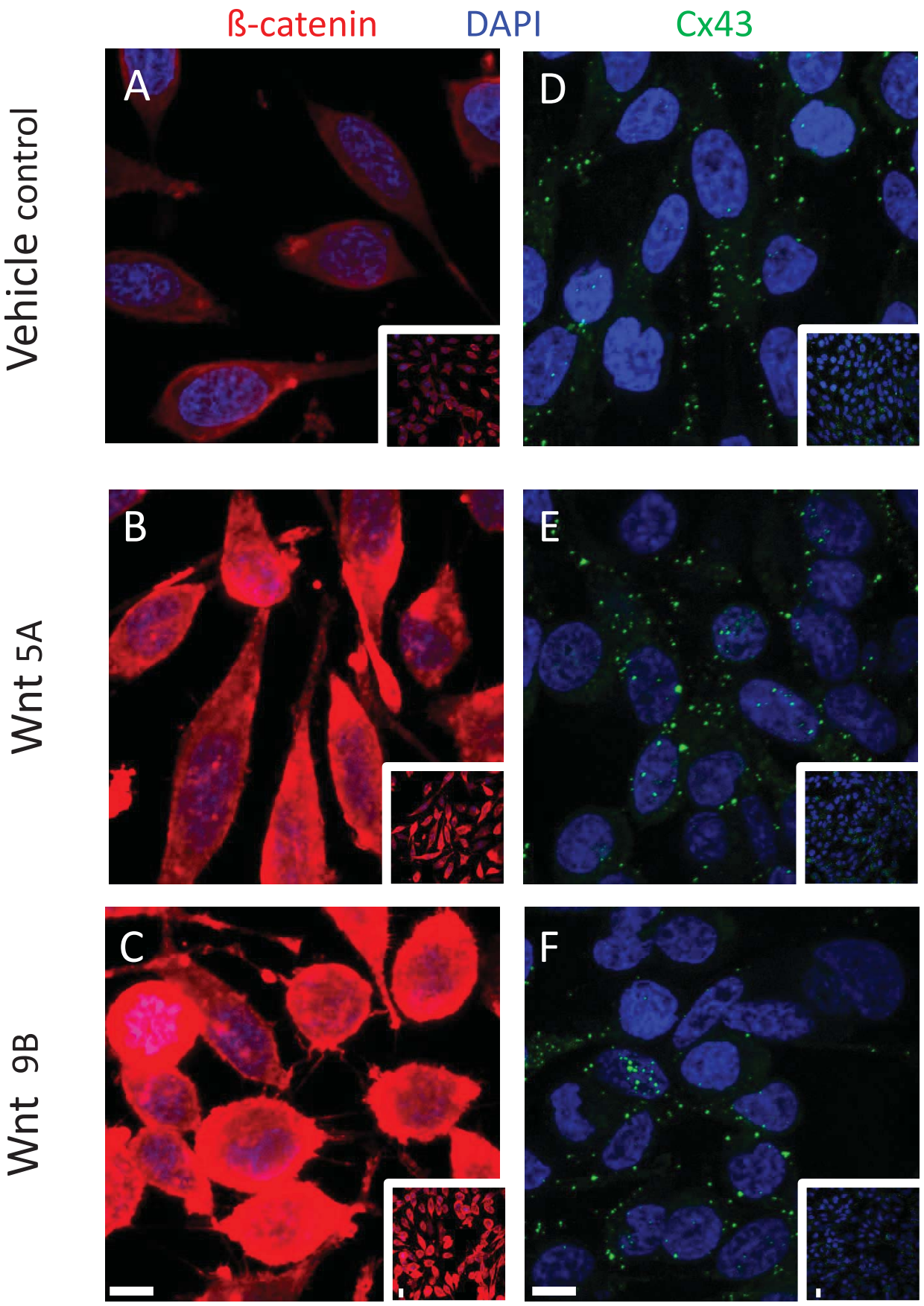

Fig 2

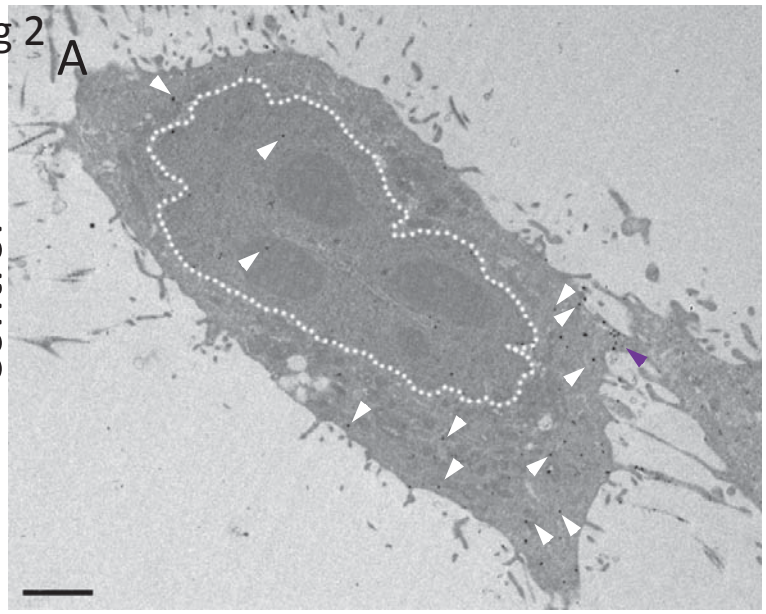


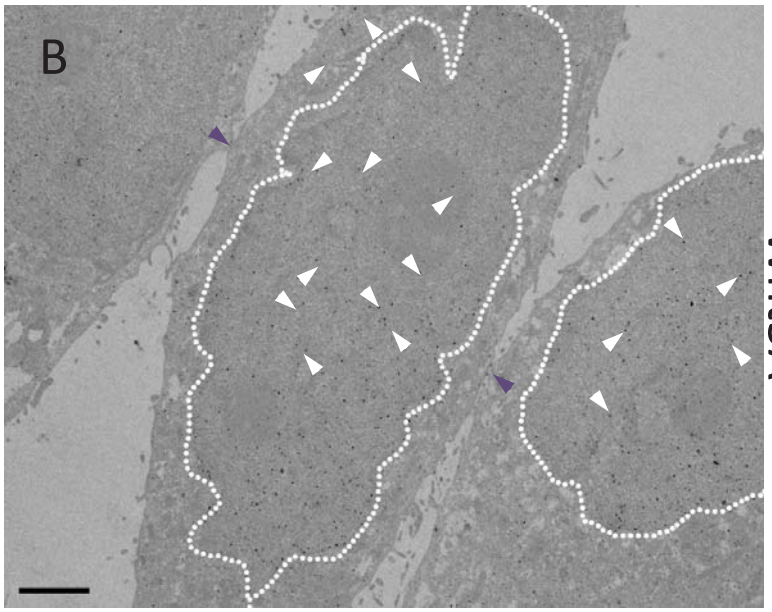


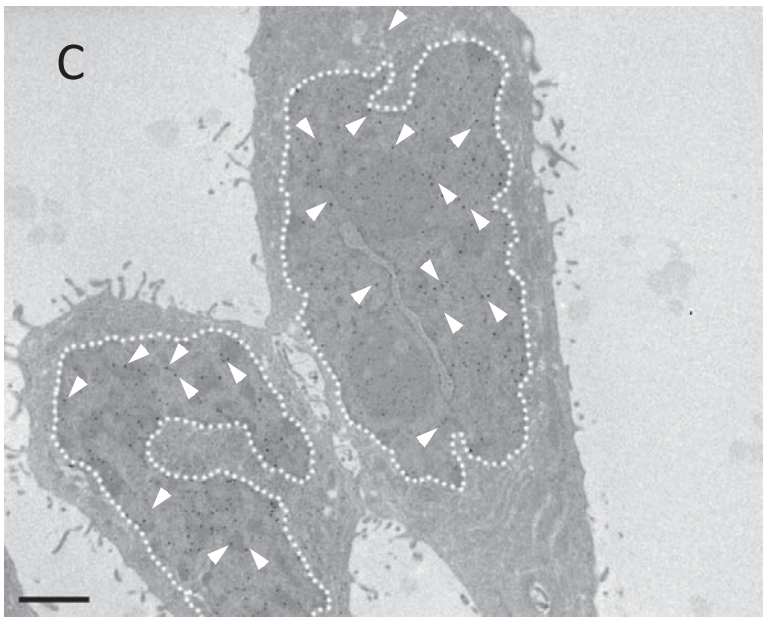


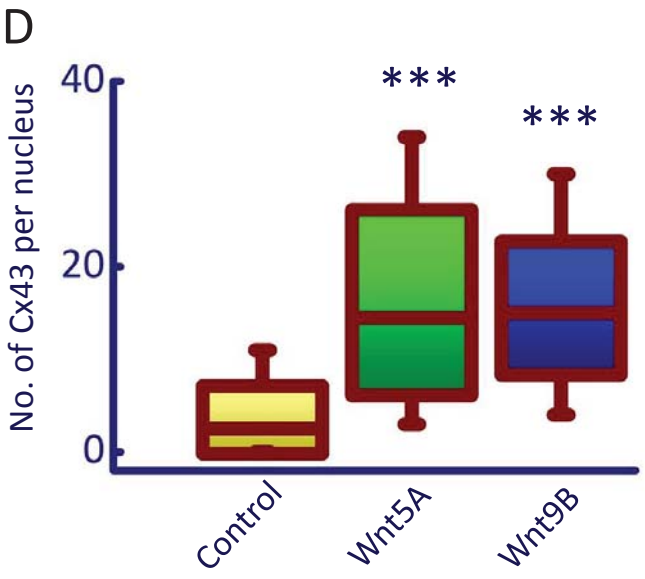

Fig 2 contd

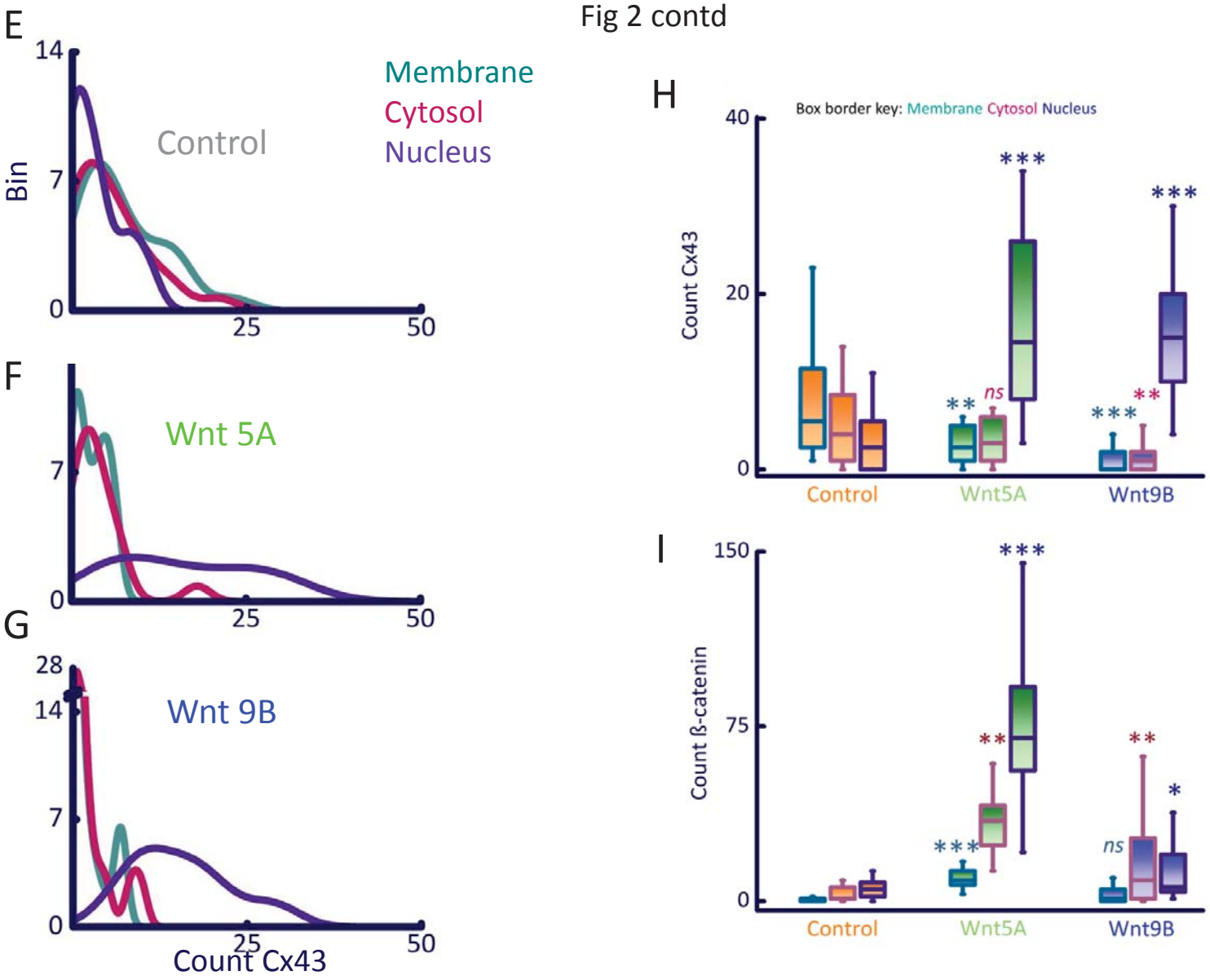

Fig 3

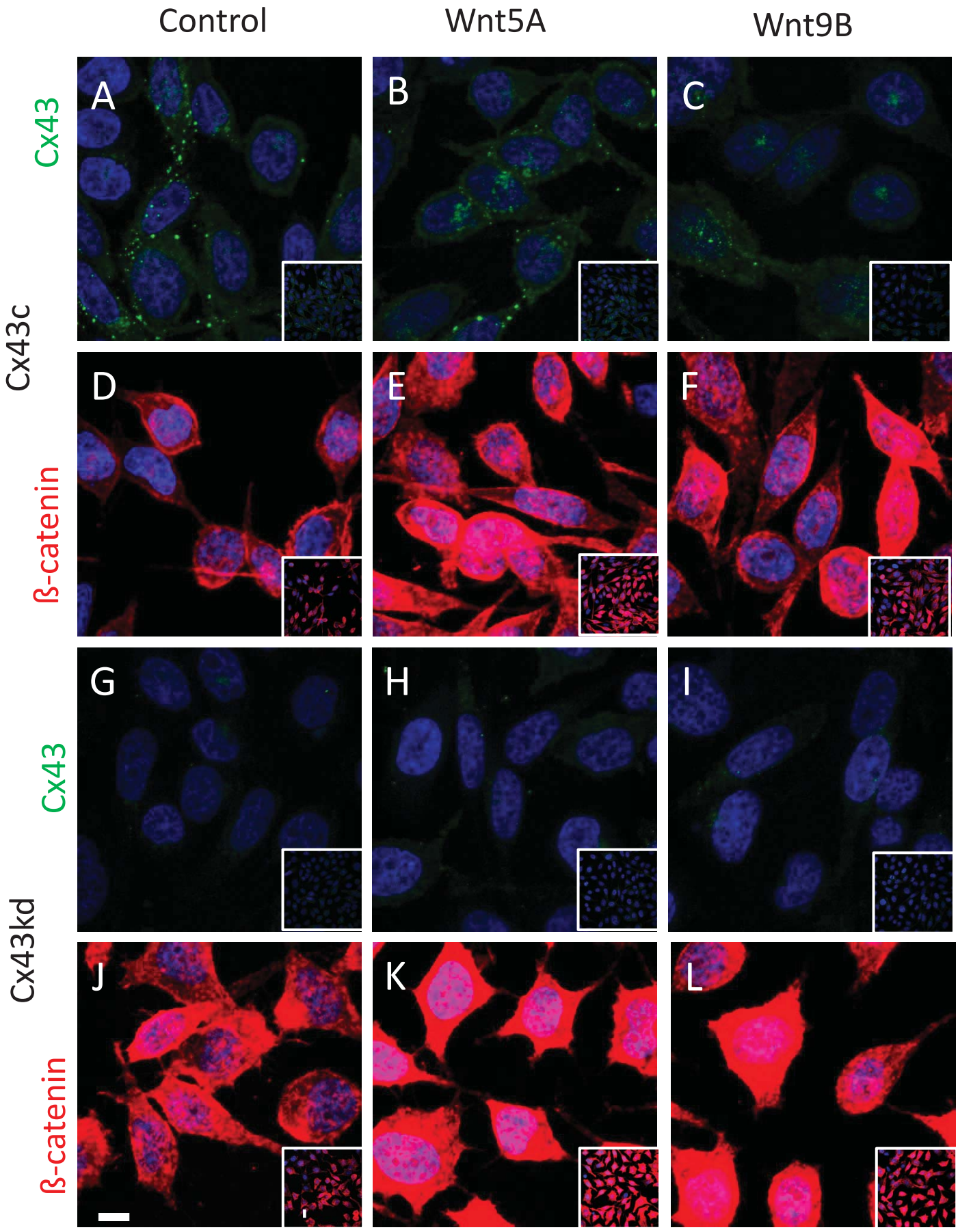

Fig 4

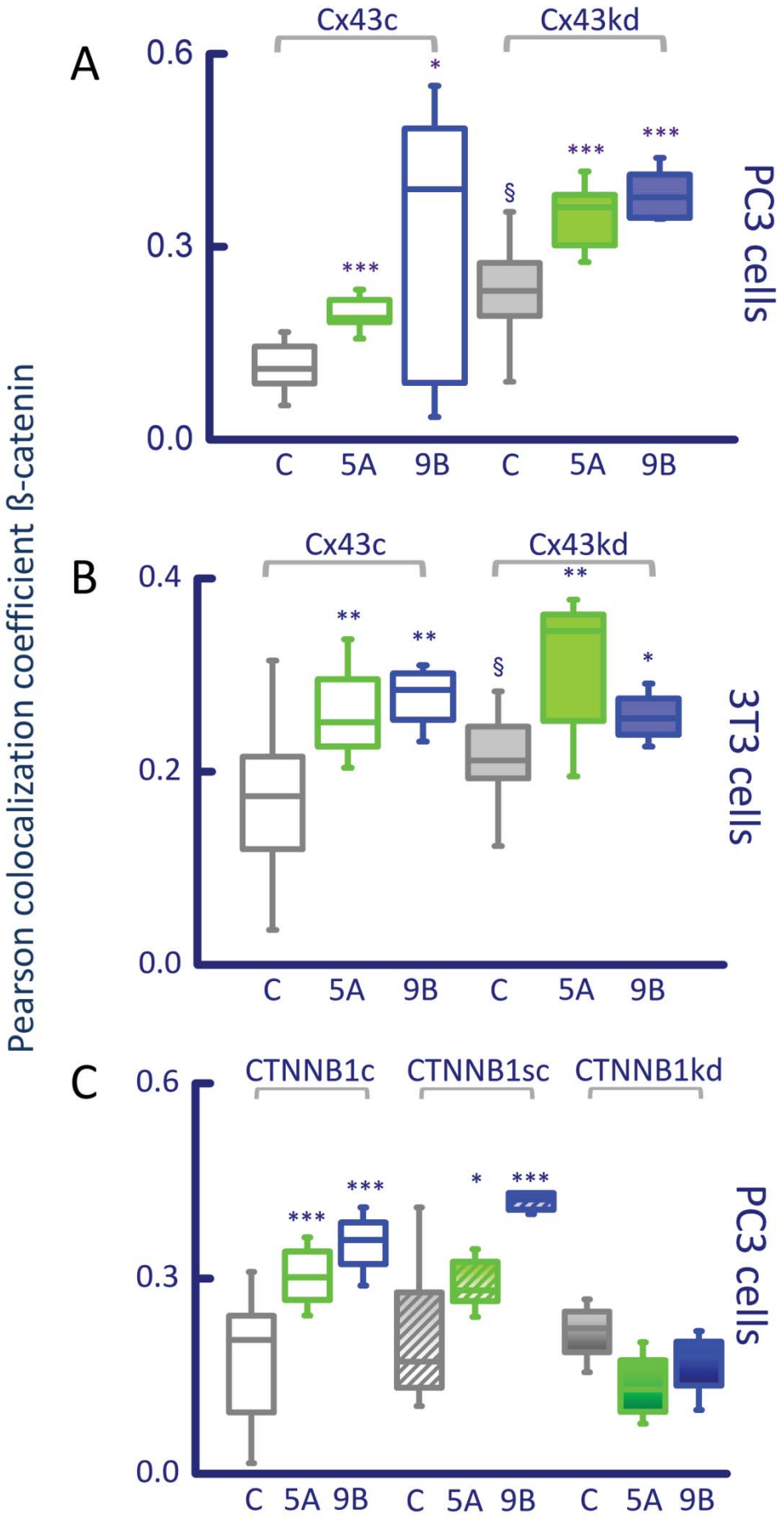

Fig 5

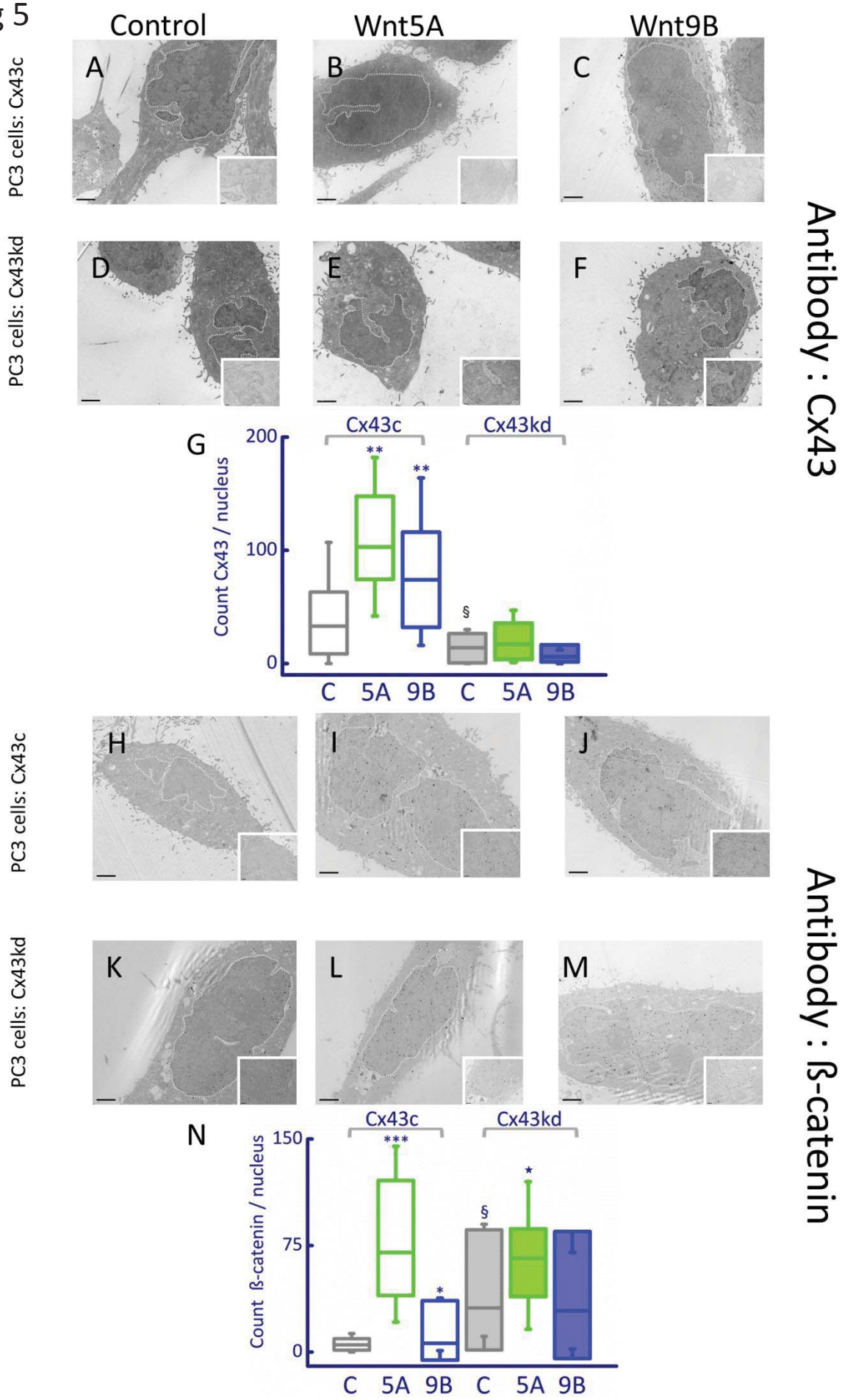

Fig 6

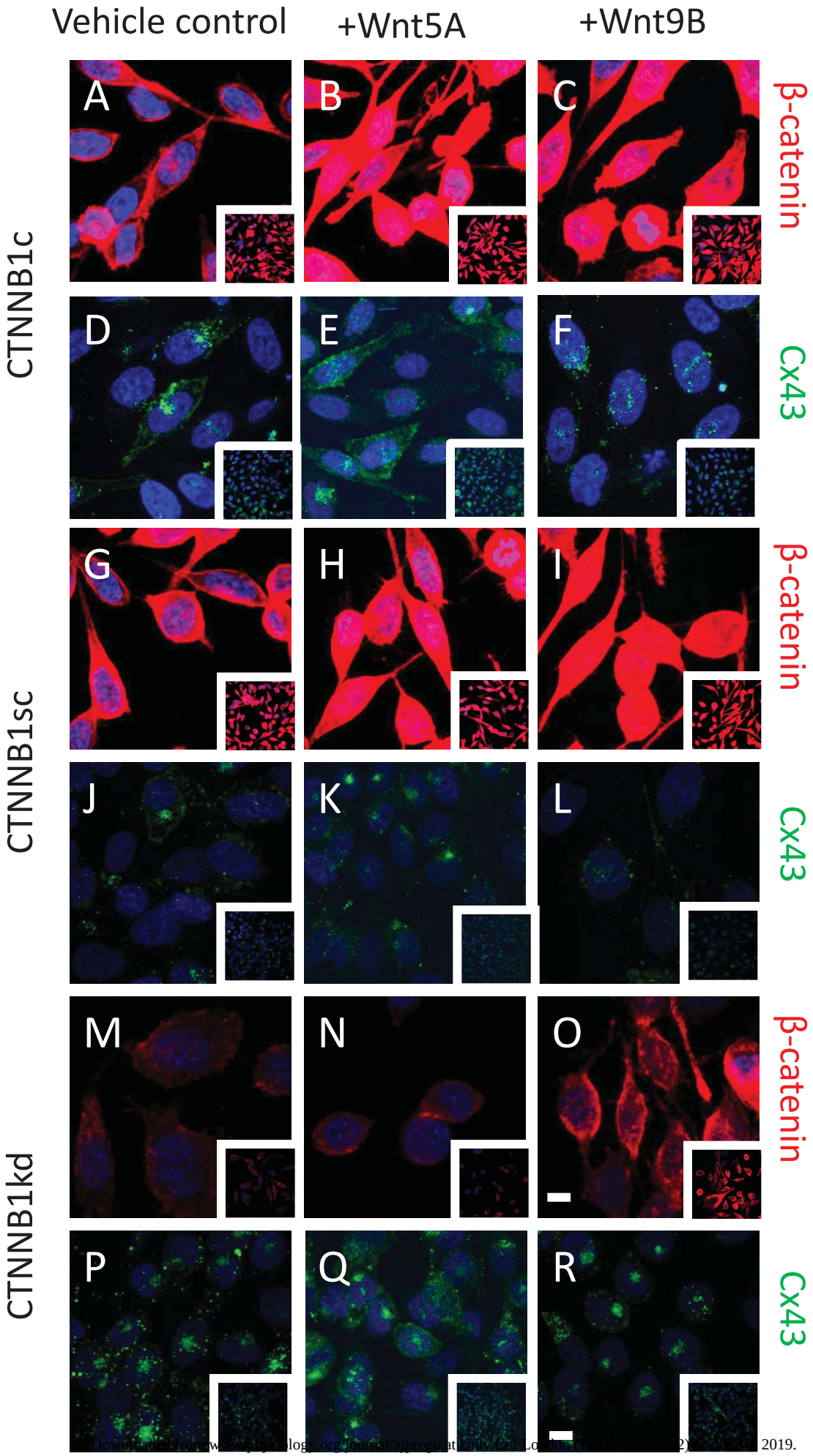

Fig 7

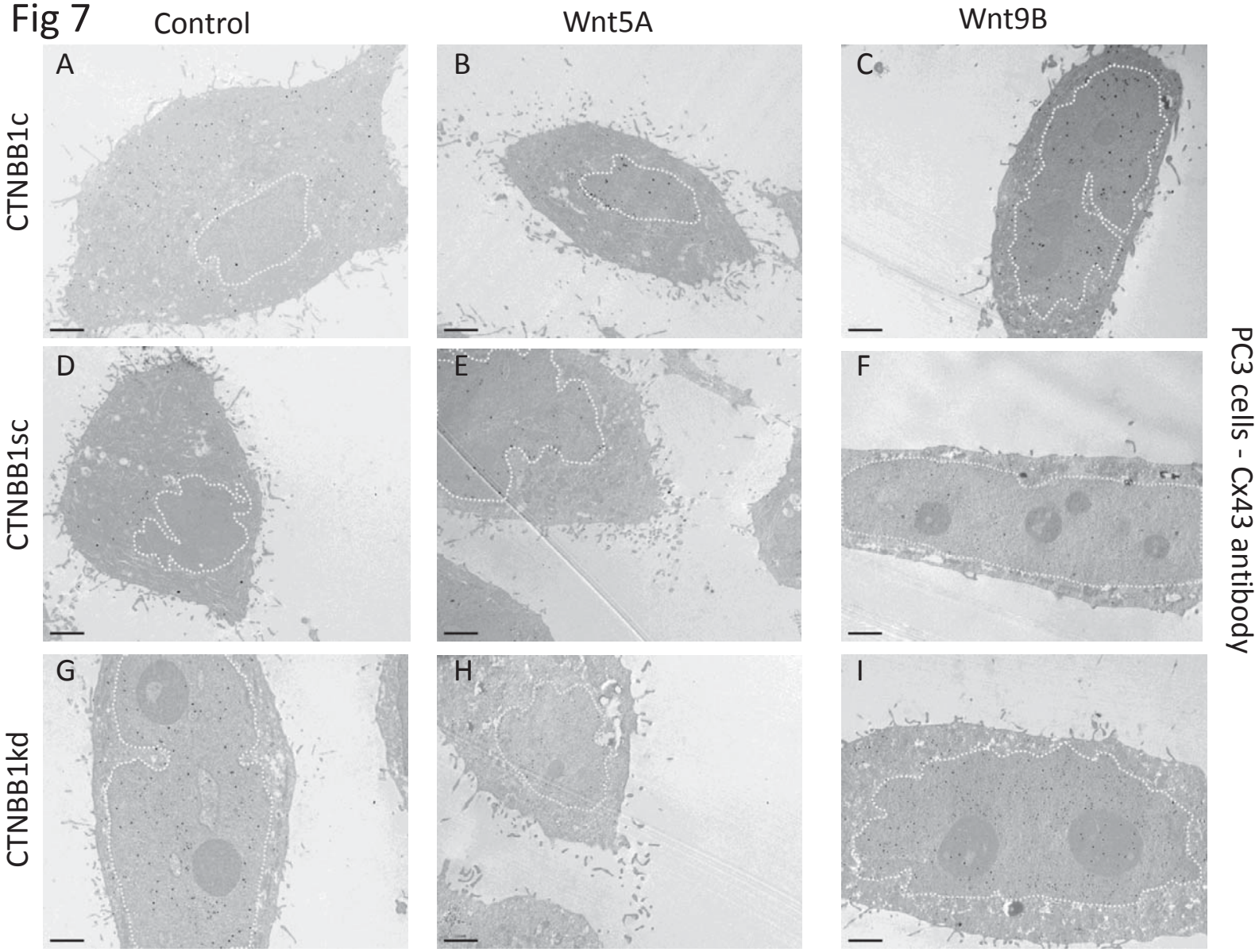

Fig 8

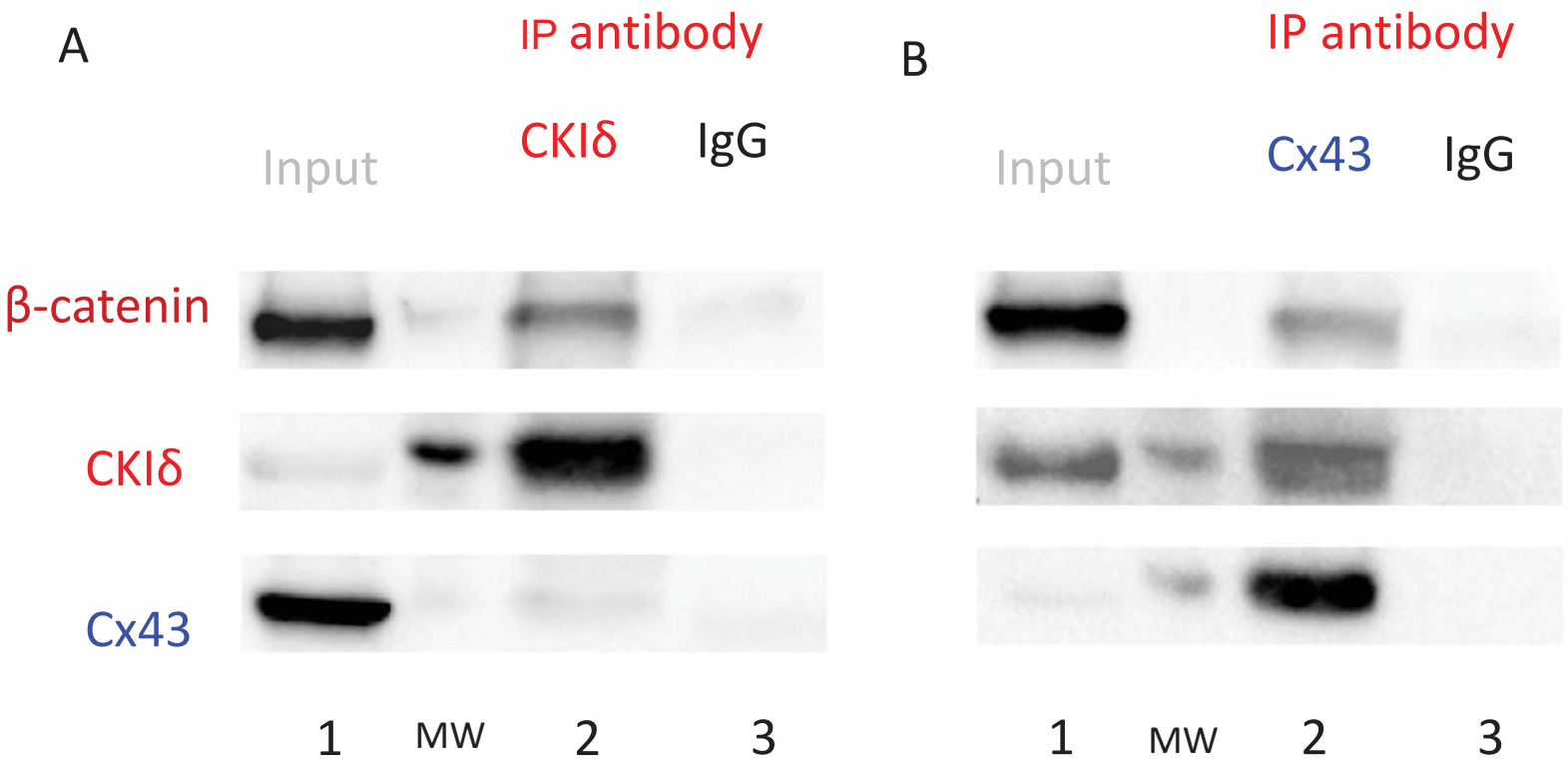

Fig 9

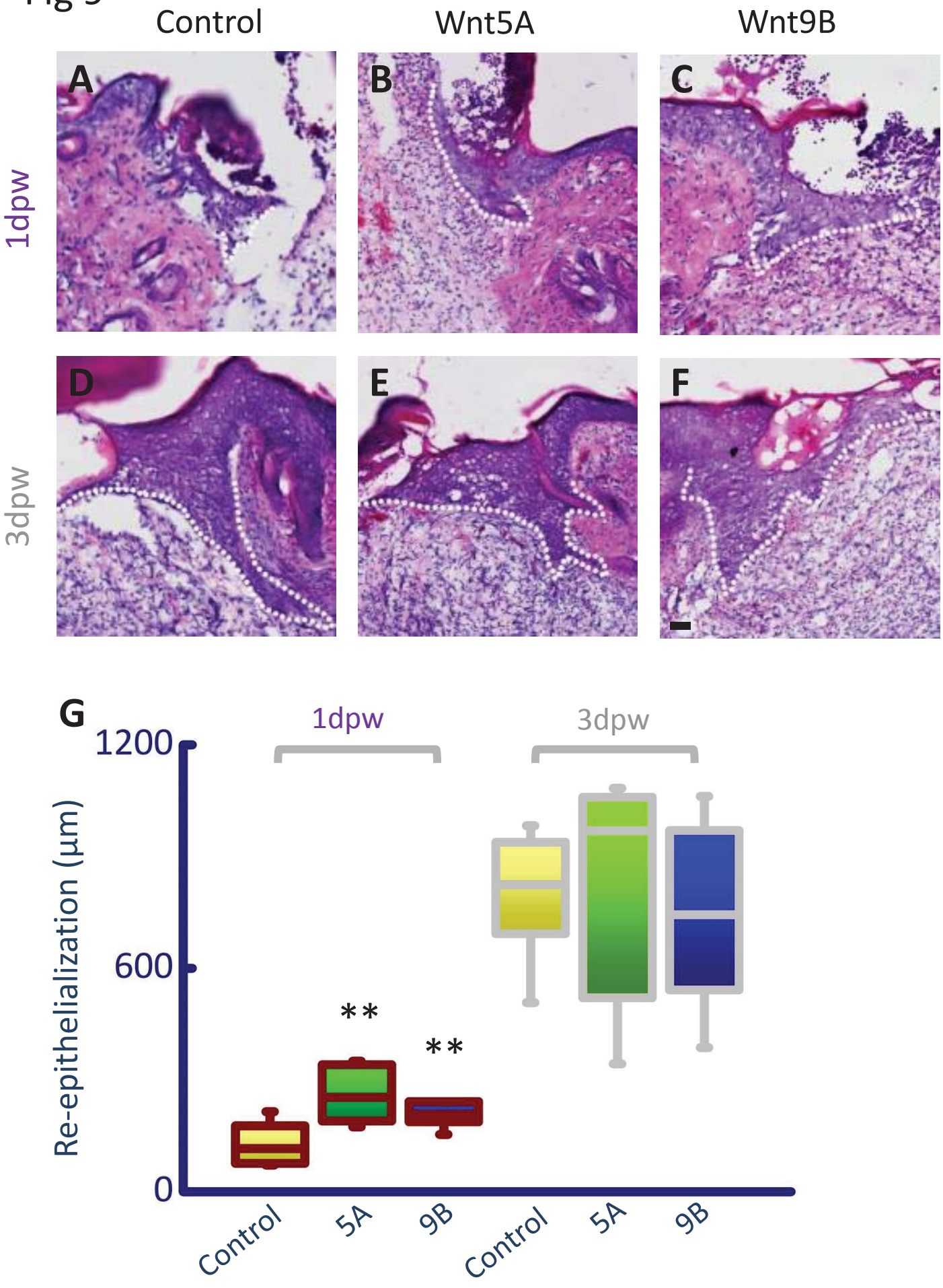

Fig 10